*Communications of the Geological Survey of Namibia, **29** (2026), 43-71*

A global review of the architecture of carbonatite complexes and its implications for melt ascent

Benjamin F. Walter[1 *], R. Johannes Giebel[2,3], Michael A. W. Marks[1] and Gregor Markl[1]

[1] Eberhard Karls University, Scharrenbergstraße 94-96, 72074 Tübingen, Germany
[2] Institute of Applied Geosciences, Technische Universität Berlin, Ernst-Reuter-Platz 1, 10587 Berlin, Germany
[3] Department of Geology, University of the Free State, 250 Nelson-Mandela-Drive, Bloemfontein 9300, South Africa

**corresponding author: <b.walter@uni-tuebingen.de>*

Abstract :- This review analyses the architecture and emplacement characteristics of 551 carbonatite complexes worldwide to address two key questions: (i) how are different geometries linked to each other genetically, e. g. early-stage radial dykes versus late-stage plugs, and (ii) does the architecture of carbonatite complexes contribute to a better understanding of the physicochemical parameters of the melts.

Carbonatite complexes are categorised into volcanic, shallow intrusive, and deep-seated types. Among the 551 studied occurrences, 48% consist primarily of single dykes or dyke swarms, while other geometries such as plugs (20%), cone sheets and ring dykes (11%), and diatreme breccias (8%) are less abundant. The remaining geometries represent various and variable features of lesser importance, such as lenses, sills, etc., which are not further discussed here. Only 20% of carbonatites lack associated alkaline silicate rocks, suggesting a genetic relationship, although exposure bias likely affects these statistics. Notably, geometries such as cone sheets, ring dykes, and plugs occur across different depth levels, limiting their use as reliable indicators of emplacement depth. Similarly, fenite halo development is influenced by local country rock properties rather than emplacement depth.

Field data from key localities, such as Kaiserstuhl (Germany), Oldoinyo Lengai (Tanzania), Palabora (South Africa), and Ardnamurchan (Scotland), illustrate the structural similarities between carbonatitic and silicate systems, including radial dykes, cone sheets, and ring dykes. However, a fundamental difference lies in the high vertical-to-lateral aspect ratios of carbonatite intrusions, which contrast with the horizontally extensive magma chambers typical of silicate magmatism. This distinction arises from the low viscosity, low density, and volatile-rich nature of carbonatite melts, which promote rapid ascent through the crust without significant ponding. Empirical and experimental data suggest that carbonatite magmas can ascend at high velocities and substantially faster than silicate magmas or even kimberlites. Their ascent behaviour closely resembles that of ionic fluids lacking silica polymerisation, which allows for fast and dynamic, jackhammer-like intrusion through the crust. Existing dyke emplacement models support this rapid, unsteady ascent process, involving episodic, self-closing pockets of melt that migrate upward in discrete pulses. These dynamics imply a wide range of vertical carbonatite pocket sizes, from metres to several kilometres, depending on melt volume and crustal conditions.

This review highlights the limitations of geometry alone to infer depth or genesis, given the overprinting effects of erosion and exposure bias. However, the combined structural, petrological, and geophysical data strongly support a dynamic ascent model for carbonatite melts. The refined "jackhammer model" emphasises the unique rheology of carbonatites and their capacity for rapid, transient ascent, without the need for long-lived, crustal magma chambers.

Keywords :- Carbonatite, Geomodel, Deposit model, Architecture, Ascent, Emplacement, Dykes

Introduction

Most carbonatites are igneous rocks that crystallised from carbonate-rich, mantle-derived melts. About 600 occurrences are known world-wide and the majority of them (80 %) is associated with diverse silicate rocks, including nephelinitic-melilititic, trachytic-phonolitic, basaltic-basanitic, aillikitic, kimberlitic and ultramafic compositions (Mitchell, 2005; Woolley and Kjarsgaard 2008; Yaxley *et al*., 2022). Most carbonatites are situated in the vicinity or within continental rift settings or occur along transcrustal-scale lineaments (Woolley and Kjarsgaard, 2008). A recent classification divides carbonatites by their predominant carbonate mineral into calcite/calcio- (sövite and alvikite), dolomite/magnesio- (rauhaugite and beforsite), ankerite-siderite/ferro- and nyererite / natrocarbonatites, with calcite carbonatites being the most common type (Schmidt *et al*., 2024, and references therein). Dolomite and ankerite-siderite carbonatites are much less common, and mostly occur as late-stage dykes or pockets within calcite carbonatites (Tappe *et al*., 2025; Schmidt *et al*., 2024, and references therein). Natro-carbonatite (containing abundant alkali-dominated carbonates, such as gregoryite and nyererite) is exclusively known from today´s only active carbonatite volcano, namely Oldoinyo Lengai (Tanzania) and the neighbouring Kerimasi (Tappe *et al*., 2025, and references therein).

Petrogenetic models for the origin of carbonatites have been recently reviewed in Jones *et al*. (2013), Yaxley *et al*. (2021; 2022), Tappe *et al*. (2025) and Schmidt *et al*. (2024). The two first order processes for the origin of carbonatites are (i) crystallisation from primary carbonatitic melts as a product of low-degree partial melting of carbonate-bearing mantle peridotites and (ii) fractional crystallisation of carbonate-bearing, silica-undersaturated magmas followed by silicate-carbonatite liquid immiscibility. The emplacement of carbonatitic magmas into the crust causes cyclic release of CO_2-H_2O-NaCl (±sulfate, bicarbonate) fluids/brines and variable metasomatic interactions with diverse wall rocks (e. g. Elliot *et al*., 2018; Giebel *et al*., 2019; Walter *et al*., 2021; Vasyukova and Williams-Jones, 2022; Schmidt *et al*., 2024). Published experimental data indicate that crystallisation of calcite, dolomite, ankerite, and siderite at crustal conditions requires alkaline, hydrous carbonate melts with 20 to 25 wt.% $(Na, K)_2CO_3$ + H_2O (Schmidt *et al*., 2024). These authors also suggest that carbonatite rocks, which are poor in these elements, are interpreted as magmatic cumulates. Moreover, based on experimental data, there is a high potential that most carbonatites found in the crust do not have a direct mantle origin (Schmidt *et al*., 2024).

Carbonatite can bear economic ore grades of a variety of commodities which are required for high tech, fertilizer and steel applications (e. g. fluorite, REE, Nb, P, Fe, Zr; Th; Mariano, 1989). Today, some 50-60 carbonatites are either mined or being under advanced exploration, representing ~10% of the known occurrences. However, exploration of carbonatite is challenging because of the complex and variable geometry, mineralogy, micro-textures and general heterogeneity of such deposits (Edahbi *et al*., 2018). Importantly, the true economic value of a carbonatite is not only related to volume and grade, but critically depends on a processable mineralogy and grain size to develop an exploration target into a mining operation. In this context, elucidating the processes responsible for the development of the observed geometry is of both fundamental and economic importance. Outcrop maps and the spatial distribution of alkaline silicate rocks derived from bore hole data and geophysical modelling constitute essential datasets for assessing prospectivity and guiding exploration activities. To secure the future supply of critical raw materials (CRM) from carbonatites, a refined and applicable model of the architecture of carbonatite occurrences based on known ore forming processes is required. This paper provides a global review of carbonatite geometries to answer the following questions:

- What is the genetic link between different carbonatite geometries (e. g. early radial dykes and late stage plugs)?
- What can be learned from carbonatite architecture about the physio-chemical parameters of the involved melts?

To develop comprehensive geomodels for carbonatites, these two problems need to be addressed. Recently, detailed geomodels for alkaline igneous rocks have been published (Beard *et al*., 2023), while a modern geomodel for carbonatites is still lacking. The geometric model of Le Bas (1987) is used for carbonatites worldwide, although it is largely based on observations from carbonatites in the East African rift, exposed at volcanic to subvolcanic levels. Frolov (1971) reviewed many on the known occurrences at that time and interpreted their plan view as representing different exposure levels of subvertical, pipe-like structures, distinguishing erupted and stuck complexes. The stuck ones likely had a sealing, and probably lost much less volatiles than their erupted counterparts (Walter *et al*., 2020, 2021, and references therein). Moreover, Frolov (1971) suggested that mineralisation style as well as the exposed alkaline silicate rock/carbonatite ratio of such structures are depth-dependent - an approach subsequently used and developed further by others (Arzamastsev *et al*., 2000; Giebel *et al*., 2017). A recent review (Simandl and Paradis, 2018) highlighted the role of orebody geometry within carbonatite-alkaline igneous rock complexes for exploration. The outcome of this previous work implies that i) architecture of the complex and alkaline silicate rock/carbonatite ratios depend on crustal depth (e. g. ring dykes as indicators for caldera formation closely above occur only in shallow complexes; Elliot *et al*., 2018) and ii) at a particular depth level, the observed carbonatite architecture can systematically vary (e. g. radial dykes without plugs → radial dykes with plugs → plugs without radial dykes, with increasing depth in a shallow intrusion cluster; Wooley, 1987, 2001, 2019; Kogarko *et al*., 1995). Hence the architecture of carbonatite complexes needs to be reviewed in detail for geomodel refinement which is the scope of this contribution.

Emplacement depth of carbonatites

Carbonatites are exposed at variable crustal levels (Frolov, 1971; Mitchell, 2005), but direct constraints on their emplacement depths are hampered by the general absence of suitable mineral assemblages that would allow for geobarometric determinations. For some occurrences, however, depth estimates have been published based on reconstruction of the eroded overburden at the time of emplacement. For Evate (Mozambique), up to 20 km depth have been estimated (Hurai *et al*., 2021), while for Palabora (South Africa) up to 15 km depth are assumed (Eriksson, 1982), possibly representing the deepest exposed carbonatites known. Based on ductile, synmagmatic deformation including some brittle components, the Swartbooisdrift-Ondoto dyke swarm (Namibia) was likely formed at the brittle-ductile transition zone (Drüppel *et al*., 2006, and references therein) and thus joins the list of deep-seated carbonatite occurences.

An alternative approach uses pressure estimates derived from isochoric projection of microthermometric data of fluid inclusions in primary minerals in carbonatites, such as apatite. This is, however, not straightforward, since such estimates represent the formation depth of the mineral that hosts the fluid inclusion, but not necessarily the emplacement depth of the carbonatite body itself - a problem which is recognised only by few (e. g. Andersen, 1987). For example, the fluid data of Oka (Canada) indicate fluid exsolution from a carbonatitic melt between 0.4-0.8 GPa equivalent to a depth of 14-29 km, which is much deeper than the exposure level of ~1 km, based on extrapolation of the regional geology (Samson *et al*., 1995). Similar problems for other occurrences are discussed in detail by Walter *et al*. (2021), who concluded that isochoric projections may be suitable to specify the formation depth of a particular phase, but can only be used as emplacement monitor for the carbonatite body, if there is evidence for *in situ* crystal growth (e. g. magmatic banding). Thus, knowledge of the emplacement level of carbonatite complexes is very limited and semi-quantitative at best. Accordingly, we distinguish three categories of carbonatite complexes in the following: (i) volcanic carbonatite complexes, (ii) shallow intrusive carbonatite complexes, and (iii) deep-seated carbonatite complexes. Apart from these, a further secondary category comprises complexes that were affected by metamorphism and/or deformation regardless of their emplacement depth.

Volcanic carbonatite complexes

Such occurrences expose effusive (e. g. lavas) and pyroclastic (e. g. lapilli stones) carbonatites, which are in some cases associated with intrusive carbonatite bodies (Fig. 1). Typically, extrusive carbonatites form parts of larger stratovolcanoes (and their

eroded subvolcanic centres) that are otherwise dominated by silicate rocks, or they occur as tephra cones, tuff rings, diatremes or maar-type volcanoes (Rosatelli *et al*., 2007; Woolley and Church, 2005; Stoppa *et al*., 2016). Carbonatite-bearing stratovolcanoes eroded to subvolcanic level occasionally expose ring dyke and breccia structures (Elliott *et al*., 2018, and references therein). Important examples include Oldoinyo Lengai (Tanzania), Monte Vulture (Italy), Kaiserstuhl (Germany), Catanda (Angola), Fort Portal (Uganda), Xiluvo (Mozambique), and some Mongolian carbonatites (e. g. Campeny *et al*., 2014; Dawson, 1962; Hay and O'Neil, 1983; Keller and Krafft, 1990; Petrovsky *et al*., 2012; Rapprich *et al*., 2024; Shu and Liu, 2019; Stoppa and Woolley, 1997; Von Knorring and Du Bois, 1961; Woolley and Church, 2005).

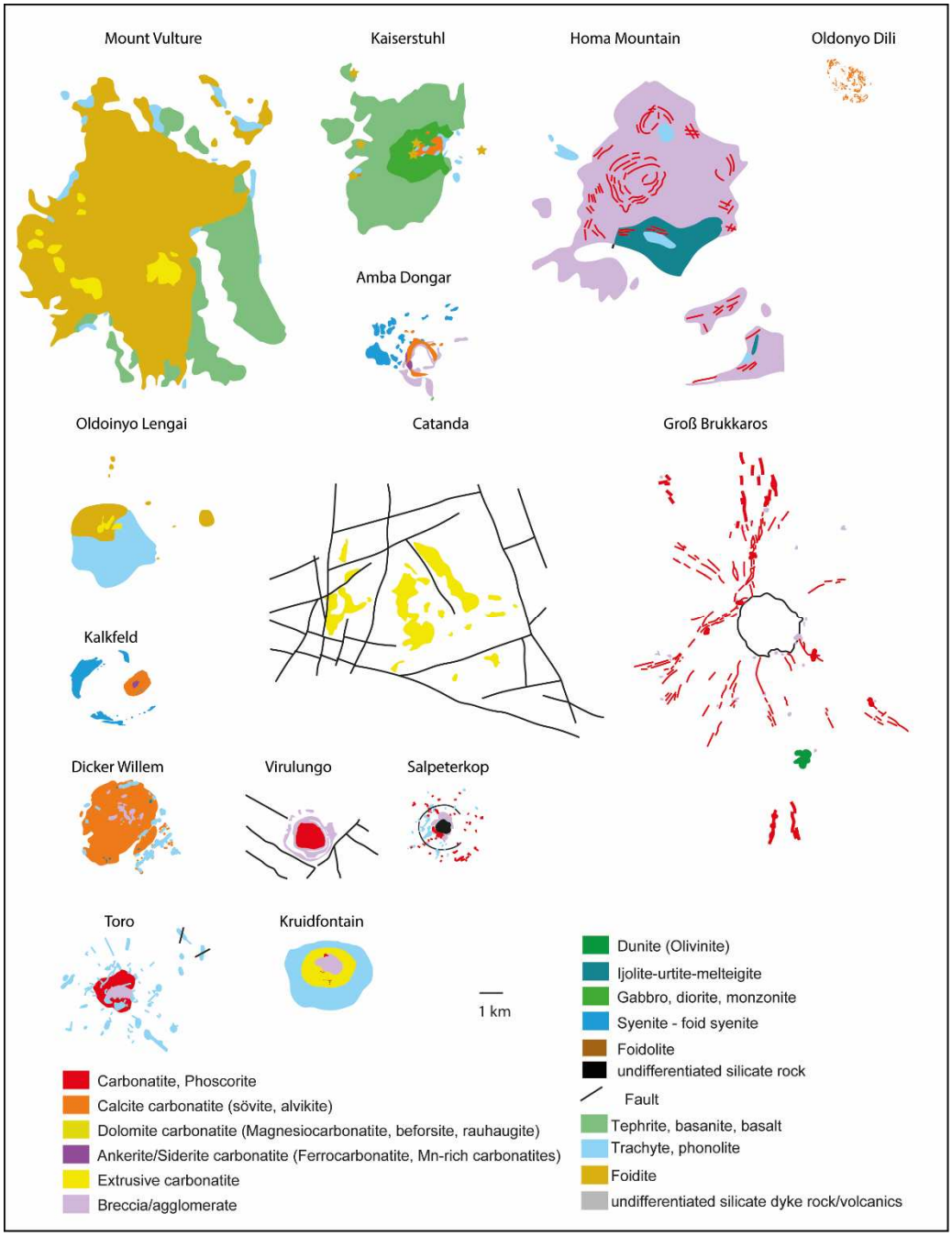

Figure 1. Compilation of exemplary volcanic carbonatite complexes, including the subvolcanic exhumation level (Verwoerd 1967; Braunger *et al*., 018; Walter *et al*., 2018; Woolley 2001, 2019)

Shallow intrusive carbonatite complexes

These complexes typically expose ring dyke/sill structures, cone sheets and radial dyke systems (Fig. 2). Central plug-like carbonatite bodies are locally exposed as well, while extrusive carbonatites are absent. Prominent fenite aureoles are common and in places coarse mafic to ultramafic rocks are associated with the carbonatites. Important examples are Glenover (South Africa), Alnö (Sweden), Fen (Norway), Sokli (Finland), complexes of the Chilwa Province in Malawi (e. g. Kangankunde, Tundulu, Chilwa Island, Songwe Hill), Panda Hill (Tanzania), Siilinjärvi (Finland), Arbarastakh, Seblyavr and Dalbykha (Russia), Dicker Willem and Keishöhe (Namibia) (e. g. Broom-Fendley *et al*., 2017; Walter *et al*., 2022; Kogarko *et al*., 1995; Woolley, 1987, 2001, 2019).

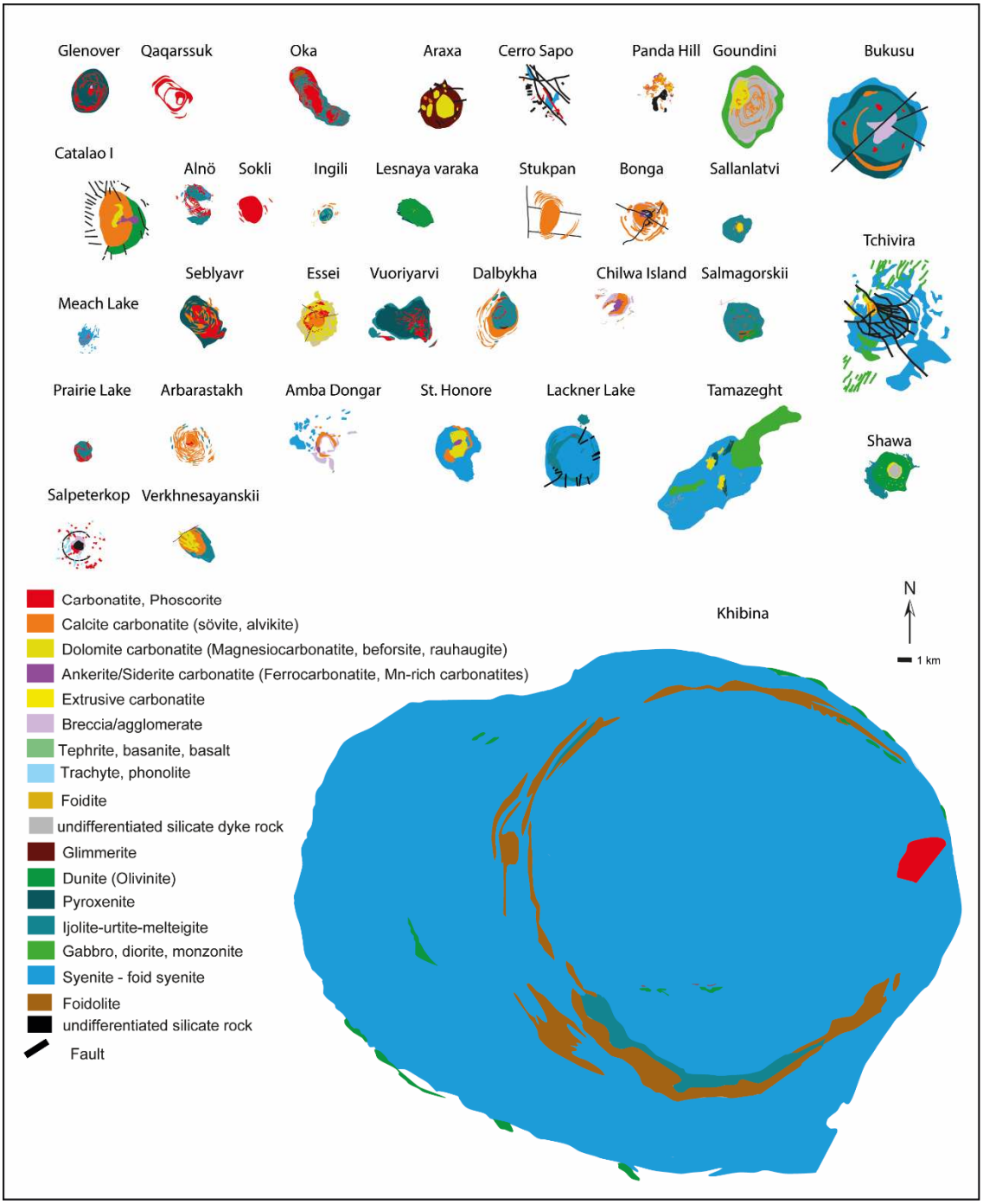

Figure 2. Compilation of exemplary shallow intrusive carbonatite complexes (Kogarko *et al*., 1995; Woolley, 1987, 2001, 2019)

Deep-seated carbonatite complexes

Intrusive carbonatites emplaced at deeper crustal levels (i. e. >8 km; Fig. 3) are not very common, which is probably an effect of global erosion depths, which are mostly upper crustal. Where they occur, such structures are mainly developed as plugs, while ring dykes, sills, cone sheets and radial dyke systems are generally absent. They often show a well-developed fenite aureole and are typically associated with significant amounts of ultramafic rock (e. g. pyroxenite, dunite) and phoscorites (e. g. Palabora; Giebel *et al*., 2019a). Important examples of deep-seated carbonatites comprise Mount Weld (Australia), Evate (Mozambique), Palabora (South Africa), and the Kola occurrences including Kovdor and Afrikanda (Russia) (e. g. Epshteyn and Kaban'kov, 1984; Giebel *et al*., 2019a; Hurai *et al*., 2021). Moreover, clusters of decimetre- to metre-wide apatitite veins (minor seams of ultramafic rock) from Nolans Bore (Australia) probably represent the root zones of a transpassing carbonatite melt migrating through the deeper crust (Anenburg *et al*., 2018).

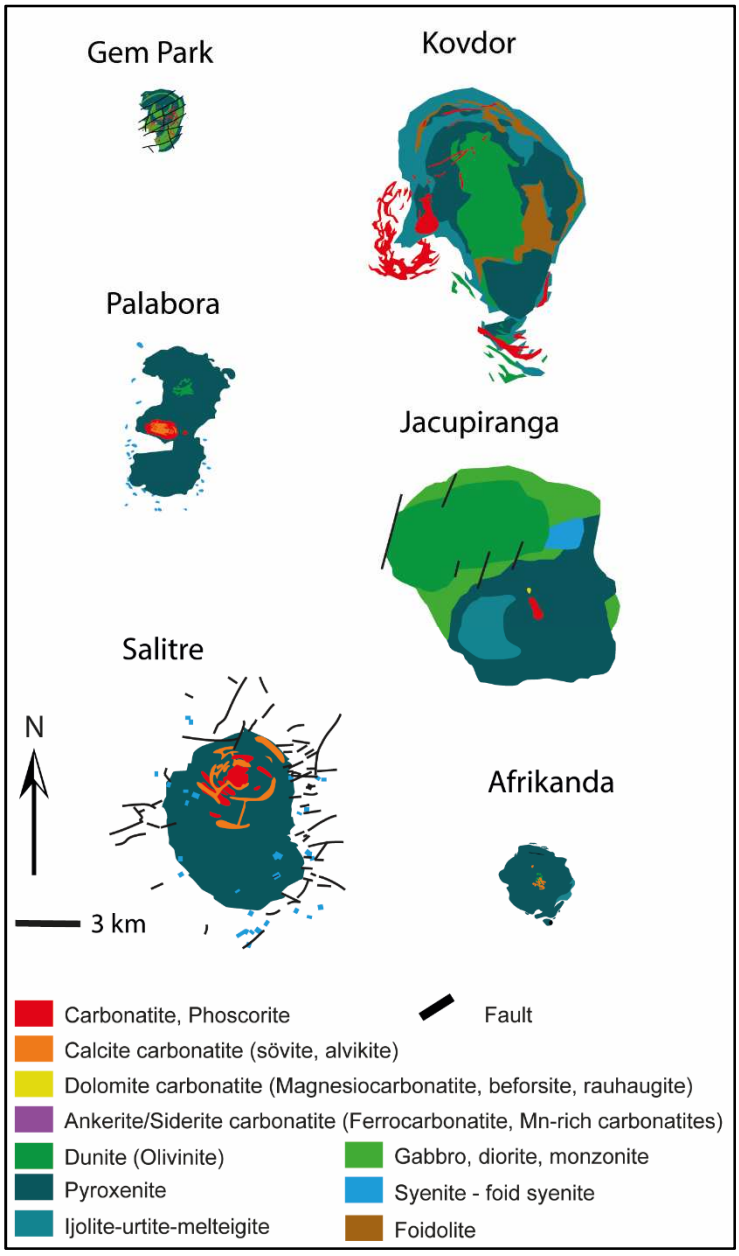

Figure 3. Compilation of exemplary deep-seated carbonatite complexes (Kogarko *et al*., 1995; Woolley, 1987, 2001, 2019)

Strongly deformed complexes

Deformation of carbonatites is not uncommon and can occur under ductile (e. g. Swartbooisdrift and Otjisazu, Namibia; Ice River, Canada; Bühn *et al*., 2001; Drüppel *et al*., 2006; Mitchell *et al*., 2017) or brittle conditions (Epembe and Glockenberg, Namibia; Bulls Run, South Africa; Walter *et al*., 2022.; Scogings and Forster, 1989) (Figs 4 and 5). Deformation may be related to local or regional faults and lineaments (e. g. Glockenberg and Otjisazu, Namibia; Bühn *et al*., 2001; Walter *et al*., 2022) or to larger-scale regional metamorphism, as at Loe Shilman, Sillai Patti, Koga, Jambil and Jawar in Pakistan (Khan *et al*., 2021), Eureka (Namibia; Broom-Fendley *et al*., 2021), the Maz Complex (Argentina; Casquet *et al*., 2008), the Newania, Sevattur, Jokipatti, Hogenakal, and Munnar complexes in India (Paul *et al*., 2020, and references therein), as well as several occurrences in Northern America (Blue River area, Mount Three Valley Gap carbonatites, Ice River Complex; Millonig *et al*., 2012).

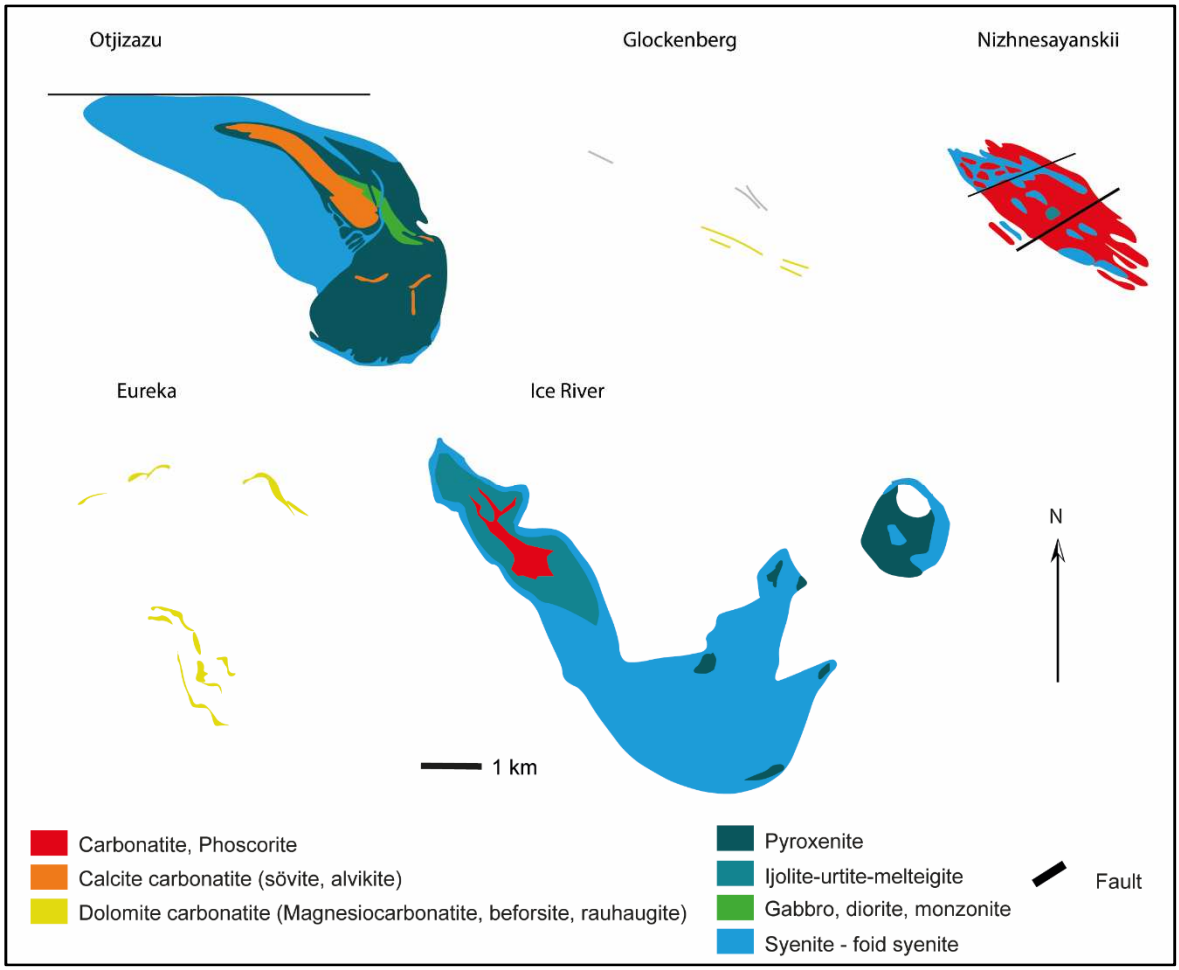

Figure 4. Compilation of exemplary deformed carbonatite complexes (Kogarko *et al*., 1995; Woolley, 1987, 2001, 2019)

3D-shape of intrusive carbonatite bodies

The general architecture of undeformed carbonatite complexes and the shape of intrusive carbonatite bodies are influenced by several factors, including physical parameters of the carbonatite magma itself (e. g. viscosity and density), the rheology of the surrounding country rocks, and the local or regional stress field (Simandl and Paradis, 2018, and references therein). Many vertically elongated and steep carbonatite bodies (plugs) are associated with radial dyke systems, cone sheets and/or ring dykes (Figs 6 and 14; Simandl and Paradis, 2018). The formation of cone sheets and ring dykes, for example, is strongly related to the stress field induced by magma ascent and emplacement. Vertical to subvertical radial dykes or subvertical to outward-dipping, partly

crescent-shaped and locally concentric ring dykes, as well as inward-dipping, concentric cone sheets can emplace (Simandl and Paradis, 2018, and references therein). In contrast, in the case of anisotropic regional (tectonic) stress exceeding intrusion-induced stress, regional dyke swarms may form (Simandl and Paradis, 2018, and references therein) that are typically related to regional lineaments and other dominant structures, such as metamorphic foliation (e. g. Lofdal, Namibia), or structures around pre-existing batholiths (e. g. Swartbooisdrift in the vicinity of the Kunene anorthosite). Finally, certain carbonatite geometries are partly influenced by the exposure level of a given carbonatite complex. For example, radial dyke systems seem to be restricted to the top of ascending carbonatite plugs (Richat Dome, Mauritania; Gross Brukkaros, Namibia) at variable depths, whereas cone sheets exclusively occur at subvolcanic emplacement levels (Kaiserstuhl, Germany; Teufelskuppe and Keishöhe, Namibia).

Figure 5. A) Movement on the Okahandja lineament (Namibia) leads to ductile deformation in the Otjisazu Complex on a macro-, meso- and micro-scale; B) the Glockenberg carbonatite dykes (Namibia) intruded into the active Glockenberg mylonitic shear zone and were affected by brittle deformation.

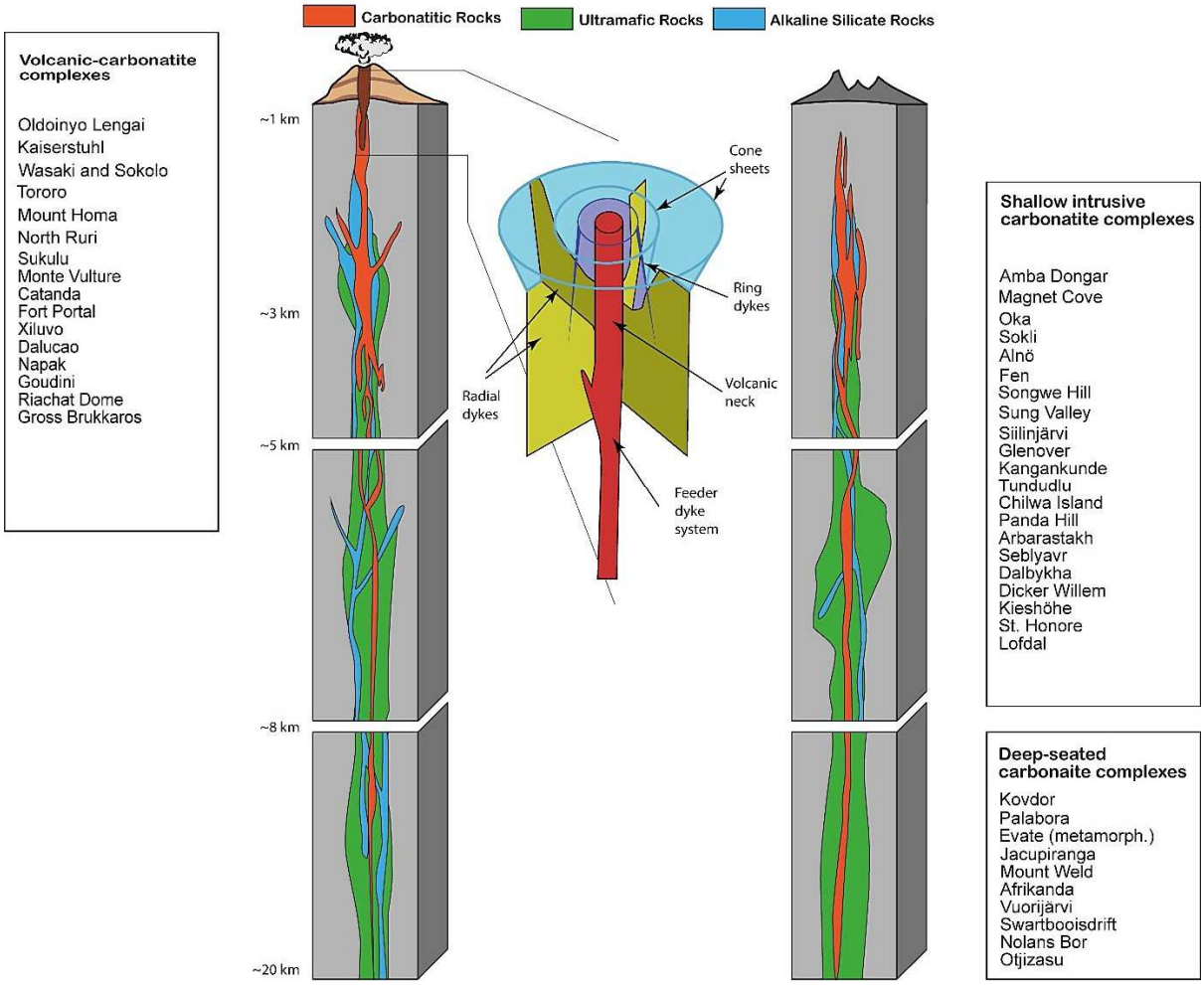

Figure 6. Modified model after Frolov (1971), Simandl and Paradis (2018) and Walter *et al*. (2021), with reference to complexes for which a reliable depth estimation exists

Regional dyke swarms (Type Lofdal)

This group encompasses carbonatite occurrences that consist of single (Fig. 7; e. g. Epembe, Namibia) or multiple carbonatite dykes (e. g. Lofdal, Namibia; Haast River, New Zealand). They lack other geometric elements, such as ring complex structures. The dykes can vary in width, mostly on the centimetre- to metre-scale (e. g. Keikamspoort and Magnet Heights, South Africa; Verwoerd, 1967); rarely they may be up to 500 m wide and traceable for several kilometres along strike (e. g. Vishnevogorskii, Russia, Chernigovskii, Ukraine; Kogaro *et al*., 1995).

Radial dyke systems (Type Gross Brukkaros)

Such localities expose (sub)vertical dyke systems that strike towards a common focal point resembling a central carbonatite plug, which may be actually exposed (e. g. Kaiserstuhl, Germany; Wimmenauer, 2003) or else hidden at deeper levels (e. g. Gross Brukkaros, Namibia; Walter *et al*., 2023). The thickness of such dykes can be variable (decimetres to metres) and may increase towards the magmatic centre (Figs 8 and 9). Well-documented radial dyke systems exposed over hidden carbonatite plugs are rare; the best examples are Gross Brukkaros and Osongombo in Namibia and Richat Dome in Mauritania (Verwoerd, 1967; Matton and Jebrack, 2014; Walter *et al*., 2023). In some cases, the radial dyke system is cut by a younger central carbonatite plug (e. g. Kaiserstuhl) or was destroyed by breccia pipe formation (e. g. Osongombo, Namibia).

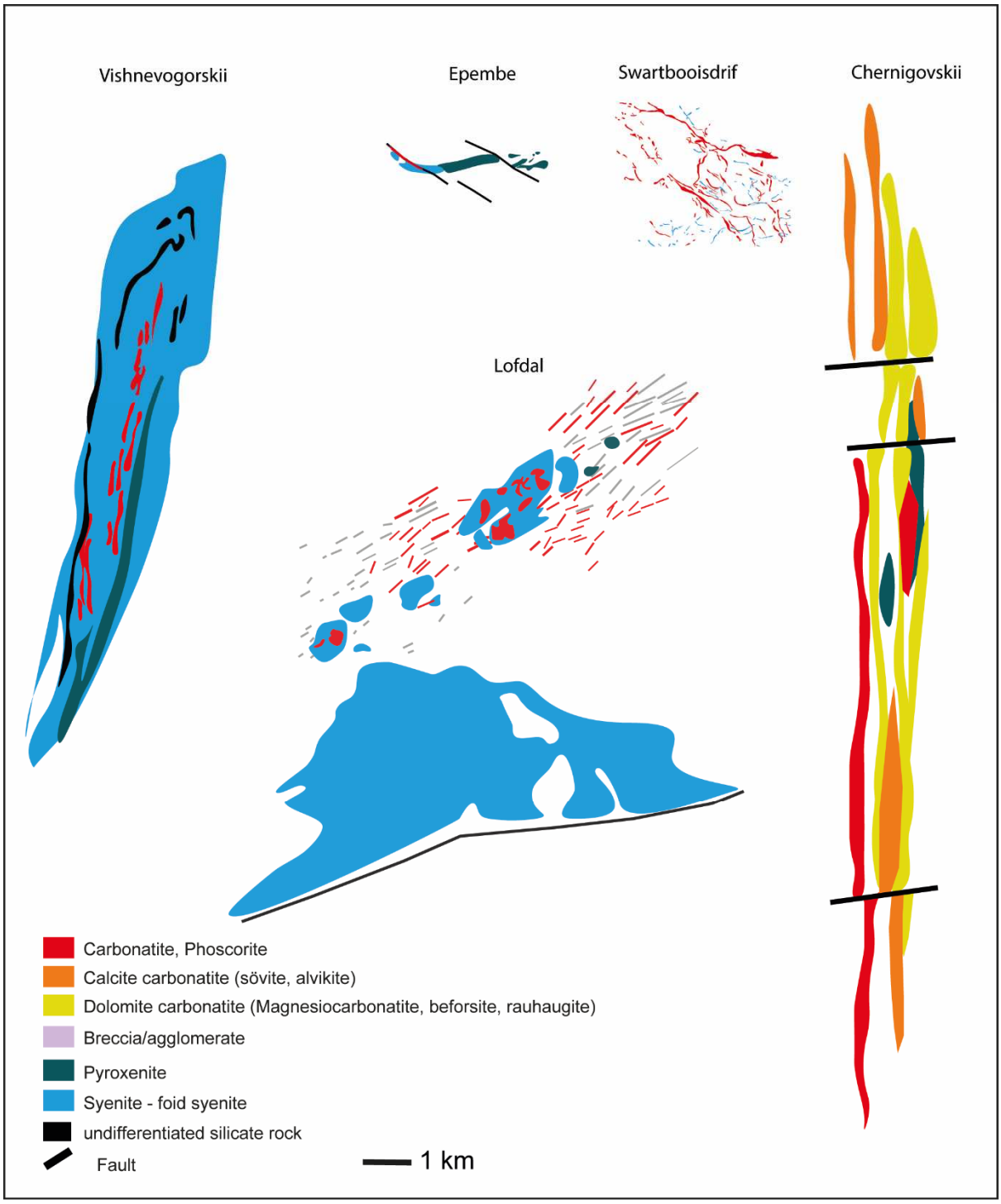

Figure 7. Compilation of occurrences classified as regional dyke swarm (Kogarko *et al*., 1995; Woolley, 1987, 2001, 2019)

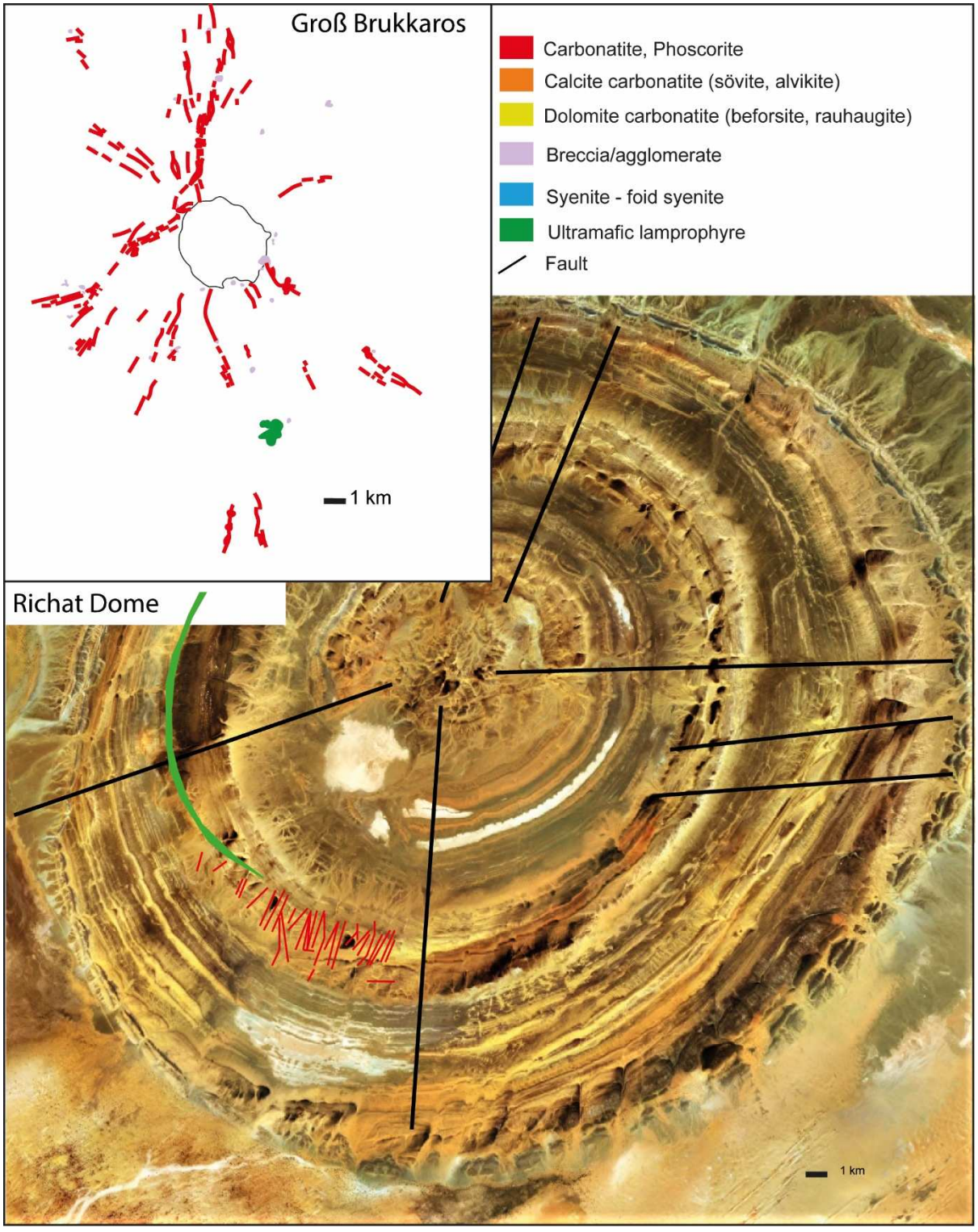

Figure 8. Occurrences classified as radial dyke swarms (Woolley, 2001)

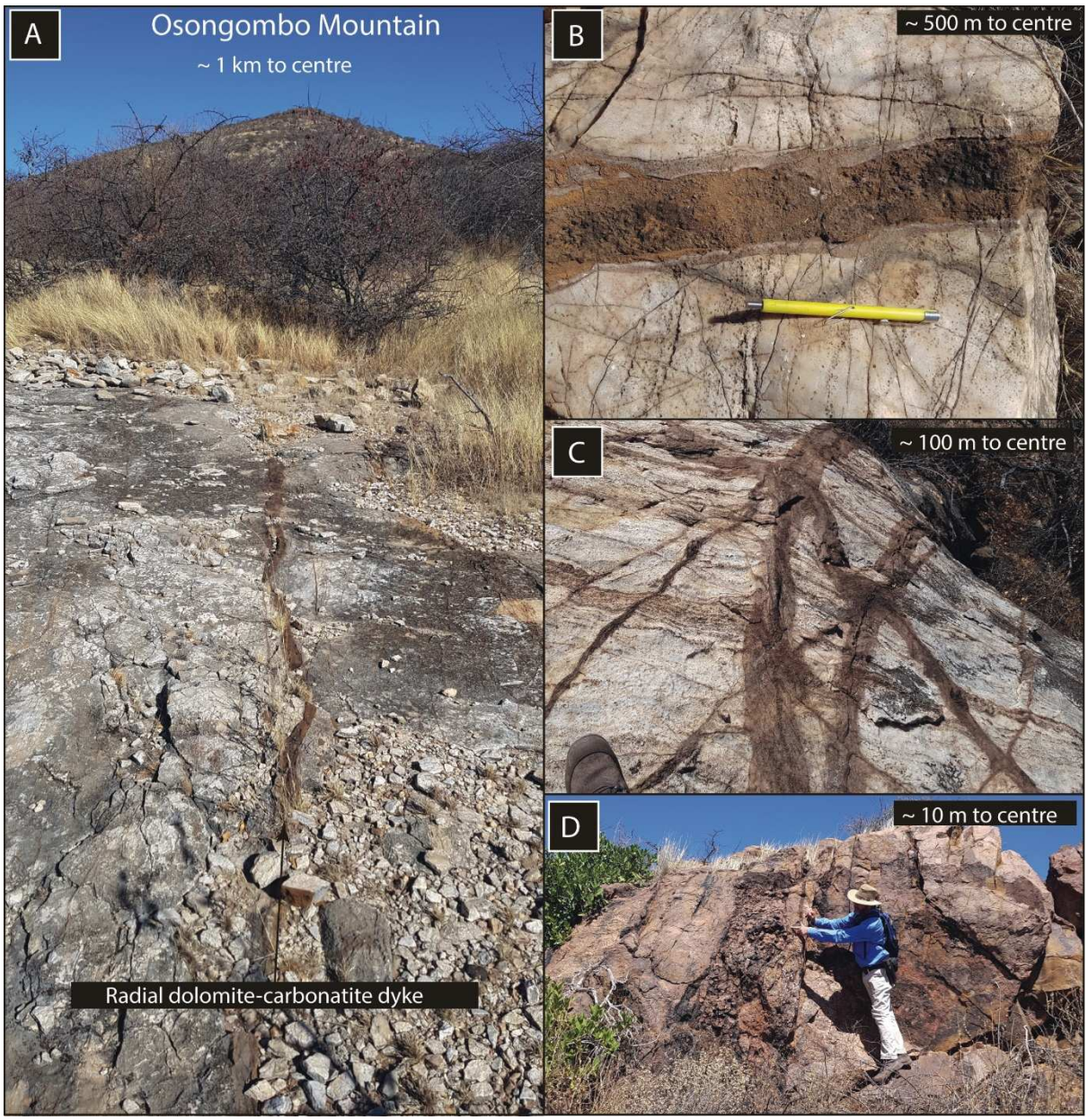

Figure 9. Radial dyke system at Osongombo (Namibia): A) small dykes of <10 cm thickness strike towards the centre (Osongombo Mountain) of the intrusion; B) with decreasing distance to the magmatic centre dyke thickness increases; C) in the direct vicinity of the centre radial dykes become more than a metre thick or form dense networks; D) in the centre of the complex the dykes end up in the root zone of a carbonatite breccia pipe.

Cone sheets and ring dykes/sills (Type Ondurakorume)

Cone sheets and ring dykes may occur at the same locality (Fig. 10). In such cases, ring dyke systems are usually cut by a cone sheet system. Cone sheet and ring dyke systems form continuous or discontinuous single or multiple circular structures of variable carbonatite lithologies, and plutonic as well as (sub)volcanic rocks (Ladisic *et al*., 2025). The width of such dykes/sills varies mostly from the decimetre- to hundreds of metres-scale. Examples of well-documented cone sheet systems include Kaiserstuhl (Walter *et al*., 2018; Giebel *et al*., 2019), Ondurakorume (Namibia; Ladisic *et al*., 2025; Figs 10, 11), Keishöhe (Namibia; Walter *et al*., 2022), Goudini (South Africa; Verwoerd 1967), Homa Mountain (Kenya; Woolley 2001), Chilwa Island (Malawi; Woolley 2001), Alnö (Sweden), Qaqarssuk (Greenland; Wooley 1987) and Arbarastakh (Russia; Kogarko *et al*., 1995). Well-docu-

mented ring dyke systems are known from Amba Dongar (India; Chandra *et al*., 2019), Glenover (South Africa; Verwoerd, 1967), Oka (Canada; Wooley 1987), Dicker Willem (Namibia; Woolley 2001) and Gardiner (Greenland; Gudelius *et al*., 2023).

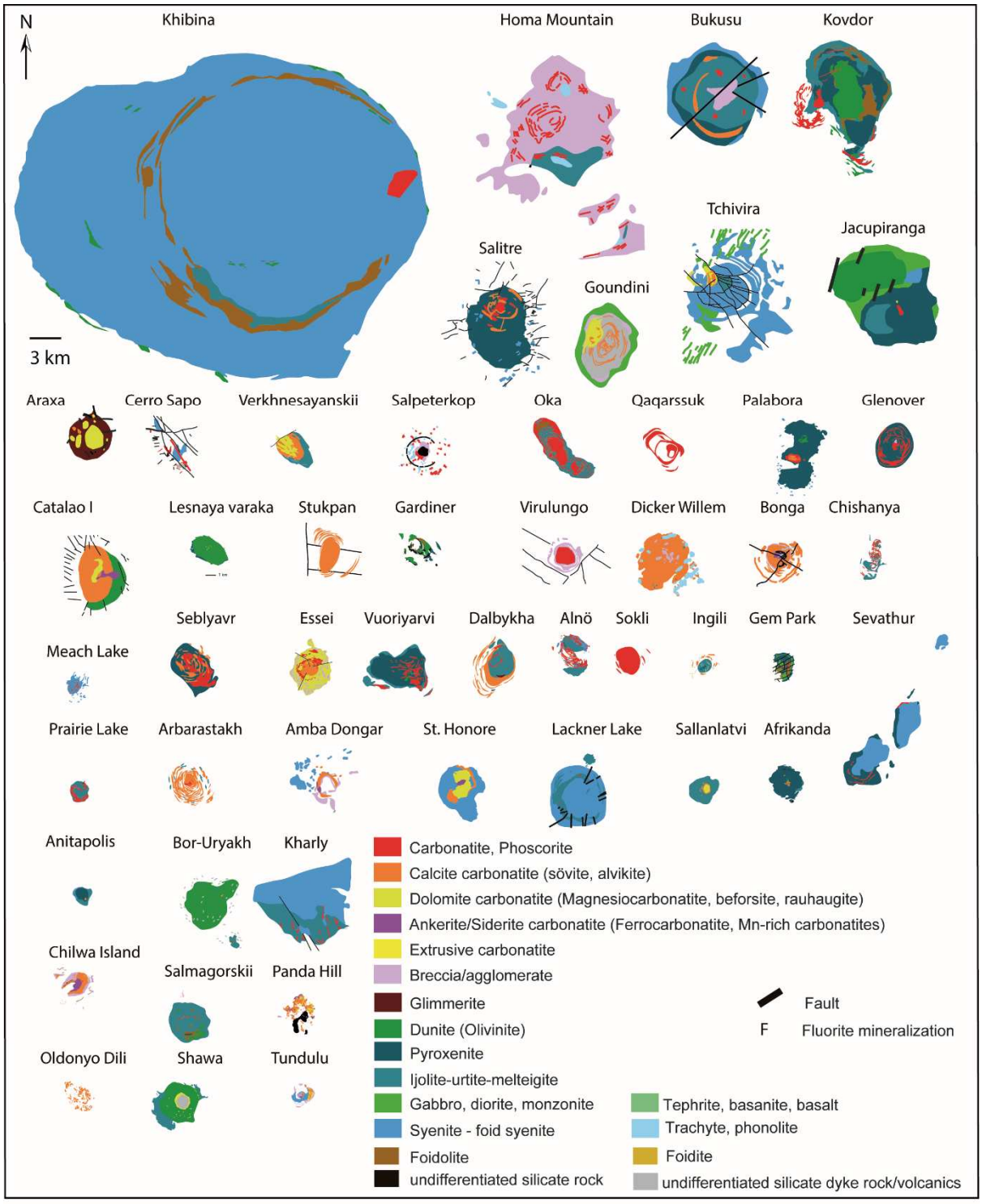

Figure 10. Compilation of occurrences with cone sheet and ring dyke systems (Kogarko *et al*., 1995; Woolley, 1987, 2001, 2019)

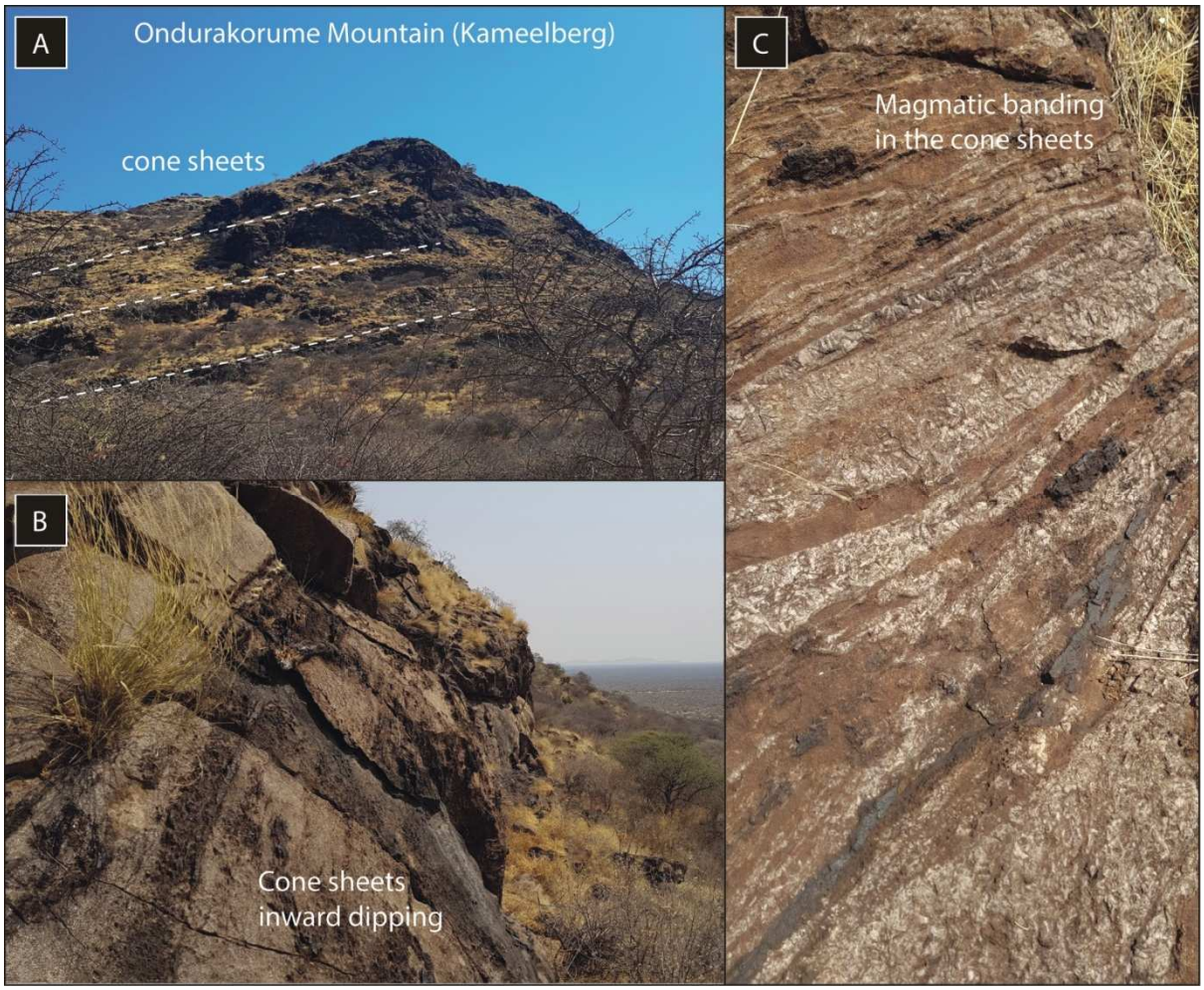

Figure 11. Cone sheets of the Ondurakorume carbonatite, Namibia: A) inward-dipping cone sheets form the entire Ondurakorume Mountain. At least three different cone sheet systems can be differentiated with younger cross-cutting older ones; B and C) calcite carbonatite cone sheet with magmatic banding

Plugs and pipe-like structures (Type Palabora)

Plugs are common features in carbonatite complexes, usually forming the main carbonatite body. Such well-developed, vertically elongated bodies can occur at the junction of transcrustal fault systems (Banks *et al*., 2019) as these represent preferred conduits for melts. In plan view, they are rounded features reaching several hundreds of metres in diameter. Such geometries have been reported from Sokli (Finland; Vartiainen and Paarma, 1979), Kaiserstuhl (Walter *et al*., 2018; Giebel *et al*., 2019), Dicker Willem (Reid *et al.*, 1990), Oka (Canada; Woolley 1987), Palabora and Spitzkop (South Africa; Verwoerd, 1967), Iron Hill (USA; Nash, 1972) and Fen (Norway; Andersen, 1987) (Fig. 12).

Cumulate pockets (Type Nolans Bore)

This group does not reflect a geometry itself, but is mentioned here as a relevant part of a magmatic system. The geometry of the apatite veins at Nolans Bore (Australia) and similar occurrences is strongly linked to a deep (granulite facies) emplacement level (Anenburg *et al*., 2018) and related zones of weakness (Fig. 13). Anenburg *et al*. (2018) interpreted these apatite veins as filter-pressing products of a transpassing carbonatite magma at deep crustal levels. Therefore, the geometry of irregular veins and pockets likely reflects a cumulate fraction generated during the ascent of a carbonatite melt. Further examples are Hoidas Lake (Canada; Pandur *et al*., 2015) and Kasipatnam (India; Choudhuri and Banerji, 1976; Rao, 1976; Panda *et al*., 2015).

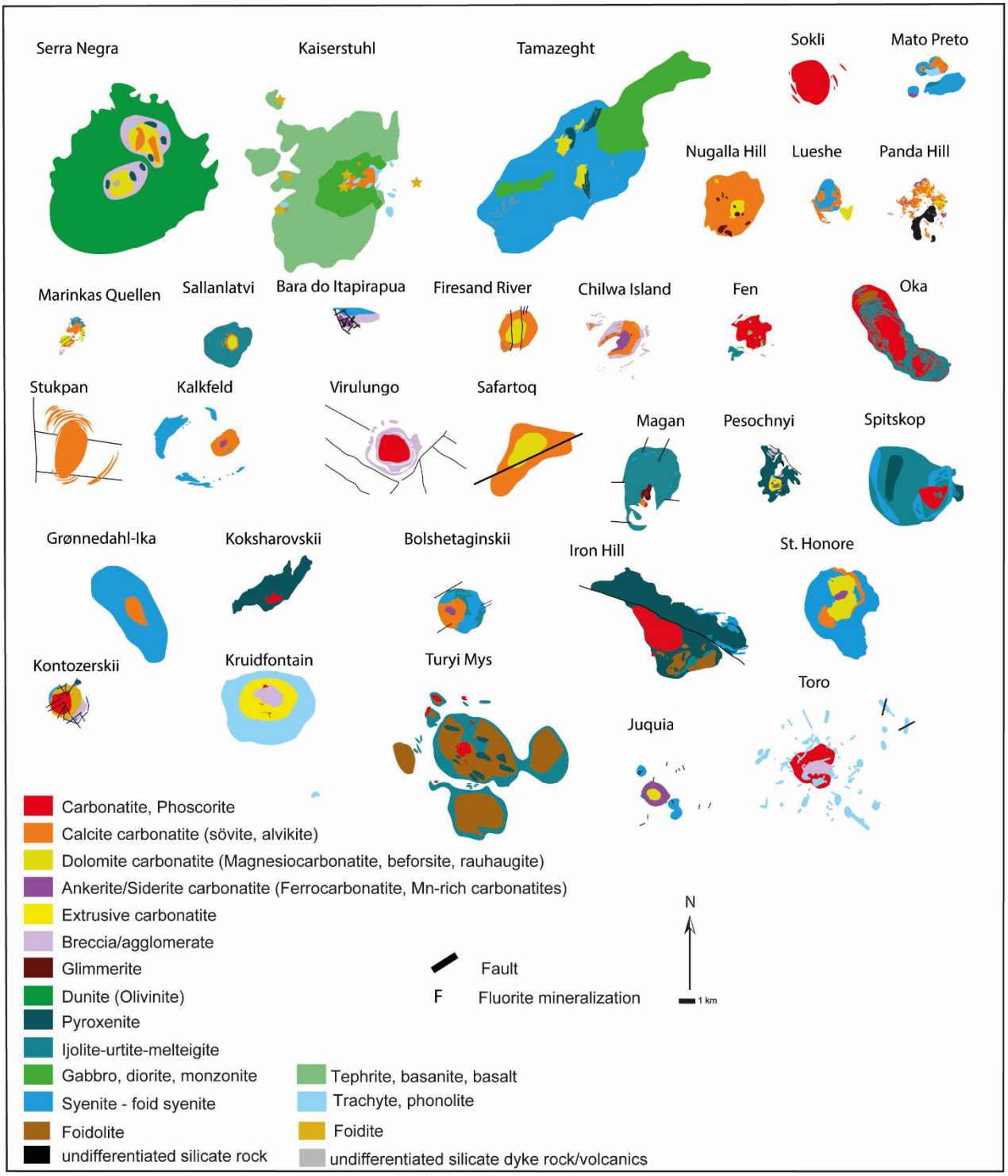

Figure 12. Compilation of occurrences classified as plugs and pipe-like structures (Kogarko *et al*., 1995; Woolley, 1987, 2001, 2019)

Approach

To evaluate the frequency of the various geometric elements described above on a global scale, this review updates the carbonatite lists of Woolley and Kjarsgaard (2008), Wooley (2019), Humphreys-Williams and Zahirovic (2021) and Schmitt *et al*. (2024) based on original and recent descriptions and published maps (supplementary information, Appendices 1 and 2).

About 20% of the 551 known carbonatites are classified as 'strongly deformed'. As deformation may alter or even erase the initial architecture of carbonatites, such bodies are not considered further. The remaining undeformed occurrences (n=459) were categorised into (i) volcanic carbonatite complexes, (ii) shallow intrusive carbonatite complexes, and (iii) deep-seated carbonatite complexes**.** For many of them, plan view maps have been digitised and plotted using the same scale, with consistently labelled lithologies. At each of these localities, the exposed carbonatite bodies were classified as (a) regional dykes swarms, (b) radial dykes, (c) cone sheets, and (d) ring dykes and plugs. It is important to note, that a single location can have more than one geometric feature, e. g. a central plug that is surrounded by a cone sheet system. This compilation provides a statistical base for a quantitative evaluation of the frequency of certain forms and shapes of carbonatite bodies in respect of relative volume and associated alkaline silicate rocks. As one complex can host more than one geometric element, the number of features (and associated lithologies) presented in the following exceeds the number of locations studied.

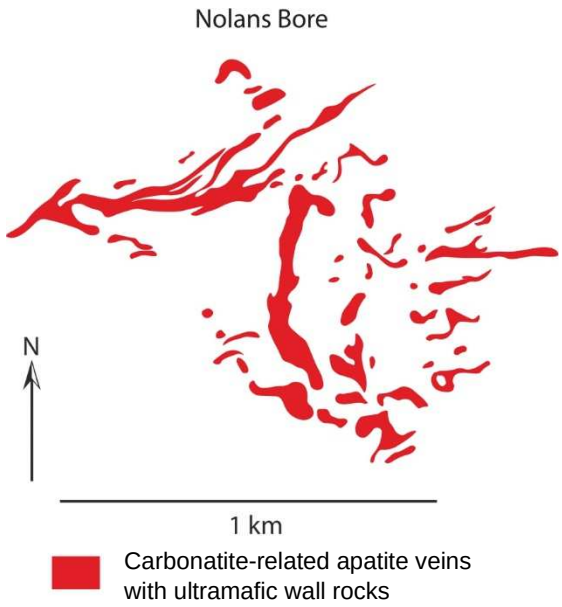

Figure 13. Apatitite pockets at Nolans Bore (Australia) as type locality of cumulate pockets

Results

What is the geometry of a typical carbonatite?

It is important to note that the geometry of carbonatites is independent of their origin (mantle versus crustal source, which is not topic of this paper); therefore, all known occurrences are considered here, not only those identified by Schmidt *et al*. (2024) as "real" carbonatites. After elimination of the deformed complexes (n=110), almost half (48%) of the remaining carbonatite occurrences, for which sufficient information was available (n=459), represent single carbonatite dykes or dyke swarms (n=260), often in association with other geometry types. Plugs are less common (n=110; 20%), followed by cone sheets and ring dykes (n=61; 11%). Sills, with only 14 descriptions (3%), are apparently rare, while subvolcanic, carbonatite-bearing diatreme breccias are described from 44 locations (8%). Occurrences of extrusive carbonatites have been updated from Woolley and Church (2005) and are described from 49 localities.

Only ca. 20% (n=118) of the known carbonatites are apparently not spatially associated with alkaline silicate rocks, which is at least partly influenced by the exposure level. Carbonatites are typically associated with foid syenites (n=171; 32%), syenites and quartz-syenites (n=154; 29%), foidolites (rocks of the melteigite-urtite-ijolite series; n=128; 24%), and ultramafites (pyroxenites-peridotites-dunites; n=156; 29%). Less commonly they occur together with lamprophyres (n=86; 16%), gabbroic rocks (n=72; 13%), phonolites (n=66; 12%), trachytes (n=55; 9%), nephelinites (n=51; 9%), melilitolites/melilites (n=30; 6%), and leucite/pseudoleucite-bearing rocks (n= 23; 4%). Please note that individual complexes

can exhibit a variety of rock associations (in addition to a combination of geometries), so that, when grouped according to these criteria, they have been counted twice or more times. Therefore, "n" combined exceeds the total number of known carbonatite complexes.

Discussion

The influence of emplacement depth on carbonatite geometry

The presence of specific geometries (except for lava flows and diatremes) cannot simply be translated into a depth categorisation, since some of the observed geometries (e. g. radial dykes) occur at various depths. Also, while it is true that, for instance, cone sheets are most common in carbonatites emplaced at relatively shallow crustal levels (Elliot *et al*., 2018), this is also the level at which most carbonatite complexes are exposed today. Therefore, interpretations of "carbonatite types" and dominant geometries, and the genesis of carbonatites are probably biased by the typical exposure level of crustal rocks. Today's exhumation situation is clearly pointing towards a dominant erosional cut of the complexes in their roof regions.

Similarly, the intensity of fenite halos surrounding a carbonatite complex cannot be taken as an indicator of emplacement depth, as several parameters are affecting the formation and extent of a fenite halo; chemical gradient to the country rocks, porosity and permeability of the surrounding rocks and fracture networks, to name just a few, can vary significantly among individual complexes at the same emplacement level (e. g. Chilwa Province, Malawi or Damaraland Province, northwestern Namibia), thus influencing alteration of the country rock.

Within the group of surficial to shallow-level carbonatites, volcanic edifices, erosional remnants of volcanoes, and subvolcanic levels of eroded volcanic systems can be observed. These include extrusive carbonatites, such as Kaiserstuhl (Germany), Oldoinyo Lengai (Tanzania) and Monte Vulture (Italy), as well as exposed conduits at locations such as Kaiserstuhl and Napak, where the inferred conduits are represented by intrusive plugs several hundred metres in diameter. Such plugs are, however, not exposed at Gross Brukkaros (Namibia) and Richat Dome (Mauritania), where only a radial dyke system of carbonatites is developed, pointing to slightly lesser (relatively!) erosional exhumation compared, for instance, to Napak (Uganda); at the latter locality a few hundred metres have been removed.

Moreover, cone sheets (Amba Dongar, Ondurakorume and Gardiner) and ring dykes (Tundulu and Homa Mountain; supplementary information, Appendix 3) are common at the same subsurficial level. On the other hand, deeply emplaced complexes like Kovdor and Salitre (Brazil; supplementary information, Appendix 3) show a very well-developed network of cone sheets, dykes and sills as well. Therefore, the architecture of a carbonatite occurrence cannot be used as a tracer for emplacement depth, with exception of ring dykes, which hint at an eroded and collapsed caldera structure.

Are "ring dyke" and "cone sheet" features always of real "dyke" nature?

A further level of complexity is related to recent research on a potential metasomatic origin of associated silicate rocks like ultramafites (Vasyukova and Williams-Jones, 2022). Numerous complexes show "ring dyke- or cone sheet-like" geometries like Kovdor (Russia) and Gardiner (Greenland; Simandl and Paradis 2018; Vasyukova and Williams-Jones, 2022; Gudelius *et al*., 2023). These contain for instance dunites or pyroxenites. It is, however, difficult to imagine that at subvolcanic levels, dunite can be crystallised as a "dyke". Consequently, a metasomatic origin might explain the observed lithologies. In this case, a lining of the ascent channel with ultramafic rocks, as interaction product between the melt and the country rocks (Vasyukova and Williams-Jones, 2022), or associated pre-existing alkaline silicate rocks could produce a similar geometry to such ring structures. If this is true, the evaluation of a shallow emplacement depth by using cone sheet systems as an argument needs to be reconsidered at least for some occurrences. Therefore, much more work has to be carried out to shed light on the process of wall-rock metasomatism and the related geometries and "pseudo-geometries" of alkaline silicate rocks and carbonatites in composite complexes.

Silicate/carbonatite ratio as indicator for relative emplacement depth

An interesting occurrence to illustrate the significance of the model provided by Giebel *et al*. (2017) is Palabora as described in Appendix 1 (see supplementary information). The main Loolekop pipe (central carbonatite intrusion of Palabora)is mined down to ~2 km without evidence of getting thinner with depth. In the southern pit, only pyroxenite was observed down to ~200 m; however, in the new levels of the southern pit, an increasing number of carbonatite dykes can be observed with depth. The same holds true for the nearby Guide Copper mine pyroxenite where carbonatite is only known from drill core. Therefore, at the same emplacement level and the same age, three carbonatites are stuck at different topographic levels. Whereas the Guide Copper mine carbonatite and the southern pit carbonatite at Palabora are stuck ~200 metres below today's land surface, the Loolekop carbonatite at Palabora reached at least the present land surface. Hence, today's level of the southern pit carbonatite records the "stopping" level in the roof zone of an ascending major carbonatite plug. The intense hydrothermal stage developed in the Loolekop carbonatite (Giebel *et al*., 2017) provides evidence that it did not extrude on to the surface, but was emplaced at a higher crustal level.

The linkage between various geometries as indicators for a pocket-like transcrustal ascent of carbonatite magmas

Radial dyke systems (e. g. Richat Dome, Napak, Gross Brukkaros; Figs 8 and 9) are probably (together with single carbonatite dykes following zones of pre-existing weakness in the country rock) the topmost expressions of carbonatitic magmas ascending through the crust (Fig. 14; Walter *et al*., 2021), consistent with deformation and updoming of country rocks at these localities (as known from mafic dykes and the experiments of Kavanagh *et al*., 2018). The radial dyke system of Gross Brukkaros (Namibia) lacks exposed cone sheets, ring dykes, or a major plug. At Alnö (Sweden), a radial dyke system is cut by a cone sheet and ring dyke system. At a slightly deeper level, the Richat Dome (Mauritania) displays a carbonatite radial dyke system, which is cross-cut by a gabbroic ring dyke. In relatively deeper erosional cuts (e. g. Amba Dongar and Oka), well-developed ring dyke systems are exposed, while radial dykes are lacking, as they probably have been eroded (Fig. 14). In numerous complexes, ring dyke systems are cut by plug-like carbonatite bodies (e. g. Dicker Willem, Oka, Kaiserstuhl; (Figs 10 and 14). In some cases, where ring dykes or radial dykes are cut by diatremes or cone sheets (e. g. Keishöhe, Tundulu or Homa Mountain), a volcanic behaviour and eruption of the system is very likely, because ring dykes develop in the context of caldera formation (Simandl and Paradis, 2018).

Because of exposure bias and/or misidentification, the deepest parts of carbonatite magmas ascending through the crust are not well documented. Recent work by Anenburg *et al*. (2018) on Nolans Bore (Australia), which is not a carbonatite *sensu strictu*, provides evidence for a "carbonatitic magma traversing the silicate-dominated middle crust". Thus, it seems likely that exposed carbonatite plugs do not extend through the whole crust, but rather show a pocket-like behaviour, whereas cone sheets and diatremes prove a volcanic behaviour at subvolcanic levels. Ring dykes and radial dykes are the precursors of the following pocket (plugs), and filter-pressed cumulates, as at Nolans Bore and similar occurrences (see supplementary information, Appendix 1), probably mark the deepest parts of an ascent track of a carbonatitic melt batch.

Regional carbonatite dyke swarms (e. g. Lofdal, Jawar, Sillai Patti, Glockenberg, Bulls Run, Eureka and Swartbooisdrift), however, probably belong to a different group of carbonatites (i. e. "post-orogenic carbonatites", Goodenough *et al*., 2021, and references therein), which follow zones of weakness along suture plains in active orogens; they show a different emplacement behaviour as their geometry is controlled by the metamorphic foliation of the country rocks or the strike and dip of shear zones. Nevertheless, it is not easy to decide if a carbonatite is intruded into a foliation or a pre-existing carbonatite was affected by tectonometamorphic events. Depending on the metamorphic path, the development of a fenite halo can be used as an indicator for pre-, syn- or postorogenic emplacement.

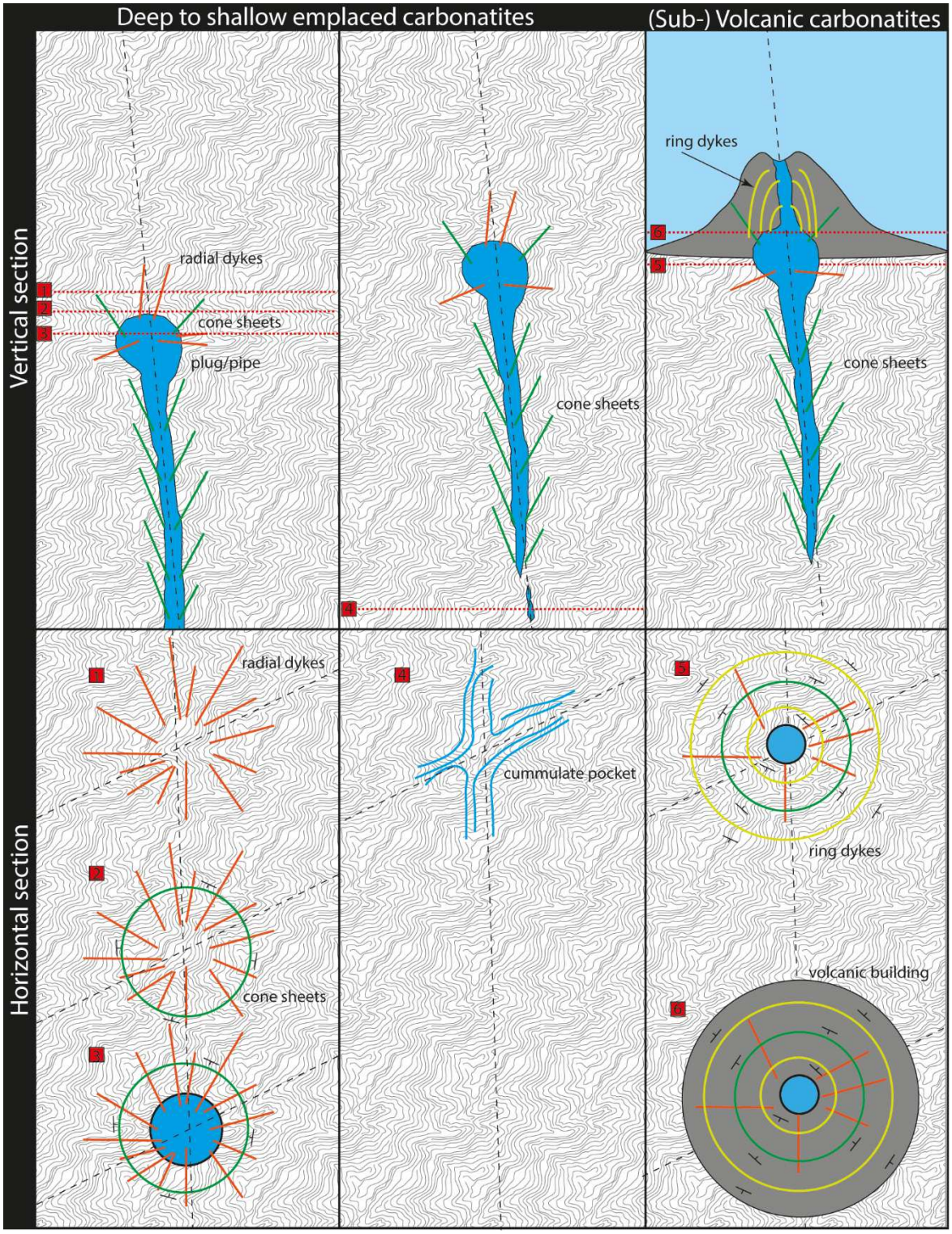

Figure 14. Schematic sketch illustrating the influence of the erosional plain on the carbonatite outcrop situation: depending on the level of erosion various architectural features can be exhumed. 1) Propagating radial dyke systems on top of a melt pocket below; 2) Slighty below the top of the radial system and above the melt pocket, radial dykes and ring dykes occur together; 3) If exhumation cuts the stuck pocket itself, a central plug can be observed on the present surface surrounded by the base of the radial and ring dykes. It is important to note that parts of the ring dyke and radial dyke system in the centre can be lost by the transpassing and emplacing main melt pocket; 4) Below the main melt pocket, the system closes, the melt is transpassing and leaves cumulates of apatite behind (type Nolans Bore). Due to the strong lithostatic forces at depth, pathways below the pockets become filter-pressed; 5) and 6) If the pocket ascends to the land surface, a catastrophic release of the melt leads to rapid emptying of the pocket and caldera breakdown. Associated with the breakdown of the caldera, cone sheet structures develop and locally are filled with the remaining carbonatite melt.

Analogies and differences to silicate systems

Carbonatitic systems exhibit structural similarities to silicate systems, including features such as radial dykes, cone sheets, and ring dykes (Simandl and Paradis, 2018). A compelling example that illustrates this analogy is the Ardnamurchan complex in Scotland, where a shallow (<5 km depth) intrusive network composed of sills, central complexes (England, 1988; Emeleus and Bell, 2005; Magee *et al*., 2013; O'Driscoll *et al*., 2006) and regionally extensive NW–SE striking dykes are exposed (Emeleus and Bell, 2005; Magee *et al*., 2013, and references therein). The cone sheets of Ardnamurchan exhibit a characteristic concentric strike pattern and inward dips ranging from 10° to 70°, steepening towards the central complex, a feature that is also observed in carbonatitic systems (Simandl and Paradis, 2018). Inclined dolerite sheets and NW–SE trending dykes intrude domed country rocks, where sedimentary strata dip outward from the central complex (Magee *et al*., 2013). These observations suggest that regional tectonic stress regimes play a key role in generating similar intrusive architectures, including cone sheets, ring dykes, and radial dykes, in both carbonatitic and silicate systems.

Despite such similarities, fundamental differences exist in the geometry of carbonatite plugs, as they typically display high vertical-to-lateral aspect ratios compared to the low-ratio magma ponding systems typical of silicate magmatism. This disparity is largely attributed to the physical properties of the respective melts—particularly density and viscosity. The low viscosity and low density of carbonatitic melts makes it impossible to build up horizontally extensive magma chambers as known from silicate systems, as lithostatic pressure will press out the carbonatitic liquids. Carbonatitic systems often lack evidence of substantial magma ponding. Given the physical and chemical characteristics of carbonatite melts—such as density, velocity, and volatile content—the formation of extensive horizontally oriented magma chambers with prolonged ponding is considered unlikely. Instead, carbonatite intrusions typically exhibit steep, semi-circular, pipe-like bodies, similar to kimberlite intrusions. Moreover, some carbonatite occurrences (e. g. Kovdor and Palabora) consist of multiple, misaligned pipe-like intrusions derived from successive pulses of carbonatitic magma, providing further evidence against the existence of a singular, long-lived magma reservoir (e. g. Kogarko *et al*., 1995; Woolley, 1987, 2001, 2019).

Rapid and turbulent ascent of carbonatite melts is supported by their physical properties. For example, due to the higher density of apatite crystals (3.1–3.2 g/cm³) relative to carbonatite melts (typically <2.8 g/cm³, commonly 2.2–2.6 g/cm³), effective gravitational separation would occur unless ascent rates are sufficiently high (Chakhmouradian *et al*., 2017; Kono *et al*., 2014).

As in carbonatitic systems, the ascent dynamics and conduit architecture in silicate systems are also governed by the physical and chemical properties of the melt, including temperature, composition, volatile content, crystallinity, and conduit wall permeability (Browne and Szramek, 2015). These parameters are comparatively well-studied in silicate systems. Key controls on ascent rates include magma viscosity and density, which are, in turn, influenced by compositional and thermal variables. Diffusion modelling based on crystal zoning patterns indicates that magmatic processes, such as magma mixing, can occur over time-scales of approximately 100 days, whereas assimilation and crystal-melt fractionation typically occur over centuries and thousands of years (e. g. Hawkesworth *et al*., 2016). Therefore, the development of shallow magma chambers in silicate systems likely requires prolonged time-scales relative to the rapid ascent observed in carbonatitic systems. Experimental data suggest a threshold ascent rate of approximately 0.2 m/s is associated with explosive eruption in silicate systems (Browne and Szramek, 2015, and references therein). In contrast, carbonatite melts are modelled to ascend at velocities of up to 65 m/s (Ernst and Bell, 2010; Genge *et al*., 1995), surpassing even those of kimberlites, for which typical ascent rates range from 0.1 to over 4 m/s (Brett *et al*., 2015), but which can also reach tens of metres per second (Sparks *et al*., 2009). Consequently, carbonatite magmas ascend more than two orders of magnitude faster than silicate magmas (Tappe *et al*., 2025; Walter *et al*., 2021, and references therein).

Analogy to mafic dyke emplacement

Mafic dyke systems have been studied for their ascent behaviour because they exert an influence on volcanic eruption styles (Caricchi *et al*., 2014, 2016; Ilyinskaya *et al*., 2017; Kavanagh *et al*., 2018). Most dykes do not erupt, as shown by field evidence, gas monitoring, and geophysical methods (Crisp, 1984; Gudmundsson, 2002). The main driver of magma ascent is buoyancy, with dyke migration described as "the release of gravitational potential energy on a planetary scale" (Putirka, 2017; Kavanagh *et al*., 2018). Kavanagh *et al*. (2018) identified four stages of magma ascent in experiments:

(1) early growth stage: dyke growth starts in the source region, with fluid jets circulating and forming a penny-shaped crack;
(2) pseudo-steady growth: a rapidly upstreaming fluid jet results in equal growth in width and length, with fluid down-welling at dyke margins;
(3) pre-eruption unsteady growth: fluid flow becomes unstable in the central jet, with acceleration towards the surface and thinning of the dyke tail;
(4) eruption stage: eruption occurs as fluid flow moves upwards and outwards, and the dyke closes with an abrupt decrease in strain.

As the experiments of Kavanagh *et al*. (2018) were performed with dyed water having physical properties like carbonatite melt (viscosity of supercritical water: ~ 0.3 Pa s, carbonatite melts: ~ 0.006-0.2 Pa s; Kono *et al*., 2014), their results and interpretations are used here as an analogue for carbonatite dyke emplacement (Fig. 15). In the context of the observed geometries in all studied carbonatite complexes and the physiochemical properties discussed above, it is probable that carbonatites behave like water-filled pockets, rapidly migrating through the crust, and closing their tail during ascent (Fig. 15). Based on the above carbonatite melt properties and the observed carbonatite/silicate rock ratios, it is possible that, depending on the entire carbonatite melt volume, carbonatite pockets between one metre and several kilometres of vertical extent can occur; smaller pockets must be generated at shallower crustal levels out of an alkaline silicate melt, or they would not have enough energy potential to move through the whole crust. This agrees with the jackhammer ascent model proposed by Walter *et al*. (2021), and therefore represents a refinement of it, in respect of a mobile pocket based on geometric arguments outlined above (Fig. 15).

Structural framework as pathways in the upper crust

Most carbonatites use transcrustal lineaments as pathways for ascent (Banks *et al*., 2019; Walter *et al*., 2021). Larger carbonatite occurrences (in particular plugs or ring dyke structures on top of them) may exist on crossings of such lineaments (e. g. Giebel *et al*., 2019). For example, the Dicker Willem and Keishöhe (Namibia) complexes occur on the transcrustal Kudu lineament (Corner, 2000; Walter *et al*., 2022). Dicker Willem is emplaced at the crossing of the Glockenberg mylonite shear zone (a Namaqua-age translithospheric shear zone), whereas Keishöhe is positioned at the junction of the Pofadder - Marshall Rocks Shear Zone and the Kudu lineament (Corner, 2000; Walter *et al*., 2022). The delamination of the orogenic root can also provide access for carbonatite melts into old suture zones, which are steepened during continent-continent collision (Goodenough *et al*., 2021; Plant *et al*., 2005). This fits in nicely with the occurrence of DARCs (**D**eformed **A**lkaline **R**ocks and **C**arbonatites; Burke *et al*., 2003) on such structures. If the ideas presented above are correct, it is possible that carbonatite melts can ascend anywhere, if the mantle reaches fertility and low-degree partial melting occurs; however, only when the melt enters the structure network within the brittle crust, they have a chance to reach the surface.

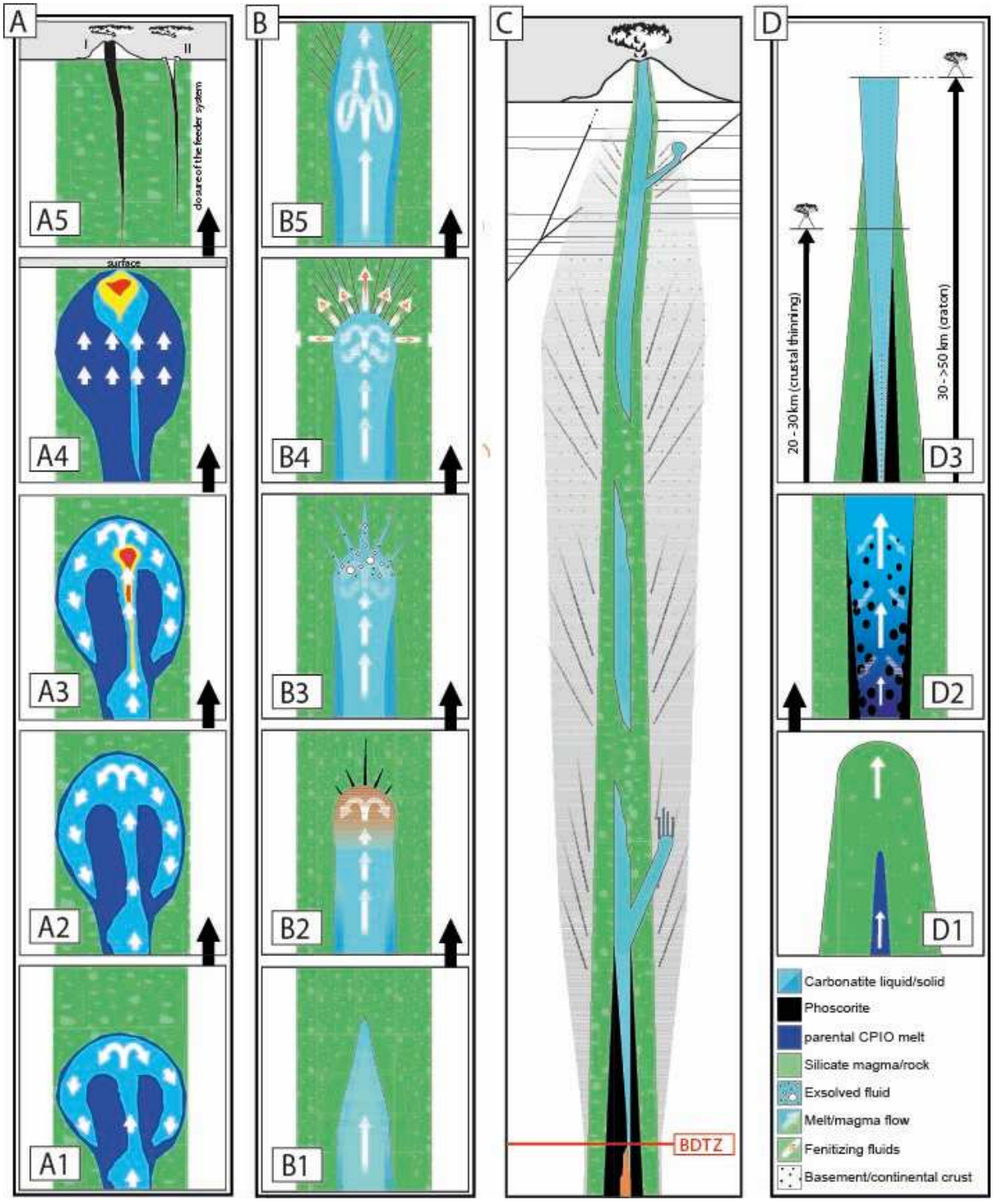

Figure 15. Refined "jackhammer" model adapted from Walter *et al*. (2021) with geometry add-on. (A) Ascent of mafic dykes, based on the model proposed by Kavanagh *et al*. (2018), is presented here as an analogue for carbonatite dyke emplacement. The schematic illustrates the rapid ascent of carbonatitic magmas. (B) Sequence of events constituting the fluid-exsolution-driven "jackhammer" mechanism: (B1) carbonatite magma reaches the terminus of the existing conduit system, forming a bottleneck; (B2) continued influx of ascending carbonatite magma leads to accumulation at the conduit end, generating fluid overpressure and inducing fracturing; (B3) expansion of fractures results in a sudden pressure drop, triggering exsolution of the fluid phase; (B4) consequently, fluids are forcefully injected into the surrounding country rock, promoting progressive expansion of fractures and cracks; (B5) this mechanism may lead to the reactivation of pre-existing fault zones, the breaching of the bottleneck, or the continued propagation of fractures until a new ascent pathway is established or the magma becomes stagnant. (C) Schematic representation of a carbonatite magma ascent

channel traversing the brittle-ductile transition zone (BDTZ): the illustration highlights varying crustal levels, with increased fracturing and enhanced fluid release at shallower depths, promoting intensive fenitisation of the overlying country rocks. The formation of phoscorite is constrained to deeper crustal levels due to its pressure-dependent nature. (D) Conceptual model for carbonatite magma ascent, modified after Giebel *et al*. (2019), which may serve as an initiation mechanism for the "jackhammer" process: (D1) a parental carbonatitic (CPIO) melt ascends along a pre-existing structural weakness utilised previously by an associated silicate magma; (D2) pressure-dependent separation of a phoscorite melt leads to a significant density contrast between the residual carbonatite magma and the exsolved phoscorite phase, resulting in jet-like ascent dynamics; (D3) conceptual depiction of characteristic rock association ratios corresponding to various emplacement levels: as magma differentiation is primarily governed by pressure, these conditions are expected to vary among continental crusts of different thickness. For comprehensive discussion of this model, refer to Giebel *et al*. (2019).

Geometry of carbonatites and their associated silicate rocks in the context of exploration

The analyses above may help to build new deposit models for mineral exploration. The model of Frolov (1971) implies a relationship between commodities and carbonatites reaching the surface and those getting stuck in the crust. His model defines a carbonatite pocket and brings the economic components into a depth relation. We consider it likely, that a carbonatite pocket on a km-scale vertical extension (depending on melt volume and pathways properties) contains apatite-rich rocks (Nolans Bore; Anenburg *et al*., 2018) at its deepest part, representing early cumulates left behind by a transpassing carbonatite magma batch. Above this level, high alkaline silicate rock/carbonatite ratios (Giebel *et al*., 2017) are expected, with enrichments in base metals such as copper (e. g. Palabora: Guide Copper mine, Otjisazu) or HFSE (High Field Strength elements) like Zr (e. g. Palabora, Kovdor). The upper parts of the carbonatite pocket, however, are strongly affected by fluid exsolution during ascent (Walter *et al*., 2020, 2021, and references therein), whereas the jackhammer-like ascent of the pocket leads to crystallisation of Nb, Ta, Sr, Ba, REE-F phases and radionuclides (U and Th). Most of the relatively deep complexes within a hypothetical pocket are low in U and Th, whereas the shallower complexes (upper part of the pockets) often show an elevated radioactivity (Frolov, 1971; Walter *et al*., 2021, and references therein). Ring dykes and radial dykes are often barren (e. g. Gross Brukkaros), but numerous complexes contain high-grade REE-Nb ores within such structures (e. g. Ondurakorume). This is most likely related to uncertainties defining a circular feature as either ring dyke or cone sheet, which also cannot be resolved by this compilation. If a carbonatite pocket reaches the surface and erupts, most of the volatiles are released and late-magmatic hydrothermal processes are prevented (Walter *et al*., 2018, 2020, 2021, 2022, 2023; Raza *et al*., 2025). Therefore, it is very important for mineral exploration to define the relative exhumation level within a carbonatite pocket in order to determine which parts of the pocket are already eroded, and what may be expected at higher levels.

Conclusions

The 3D architecture of a carbonatite complex is the result of external parameters, such as regional stress regime, and intrinsic factors like melt properties (e. g. density and viscosity). The characteristic properties of carbonatite magmas lead to a pocket-like geometry, and such magma pockets can transpass crustal levels very rapidly. The top of the ascending magma pocket is characterised by radial dykes and cone sheets, whereas ring dykes only occur in the volcanic context of caldera formation. The base of a transpassing melt batch is characterised by the closure of the pathway, and filter-pressed cumulates of early magmatic minerals such as apatite are left behind as relic schlieren and veins. The silicate rock/carbonatite ratio of a complex is a depth-related feature, with dominant ultramafic rocks occurring at higher levels. With decreasing depth, i. e. at higher levels, the carbonatite portion increases within a complex. Hence, the geomodel presented here provides a holistic view of the architecture of carbonatite complexes and can be used to identify mineralisation within an individual occurrence.

Acknowledgements

We are thankful to Aylin Polat and Kira Wolpers for their help with producing digital maps. Pete Siegfried, Andreja Ladisic, Saskia Dück, Mohsin Raza and Fadila Adamu are thankfully acknowledged for insightful discussions. Ute Schreiber and Axel Müller are kindly acknowledged for editorial guidance and constructive reviews. This study is supported by DFG (Deutsche Forschungsgemeinschaft) grants WA 3116/3-1, WA 3116/4-1 and WA 3116/15-1 to Benjamin Walter.

References

Andersen, T. 1987. A model for the evolution of hematite carbonatite, based on whole-rock major and trace element data from the Fen complex, southeast Norway. *Applied Geochemistry*, **2(2)**, 163-180.

Anenburg, M., Burnham, A. D. and Mavrogenes, J. A. 2018. REE redistribution textures in altered fluorapatite: symplectites, veins, and phosphate-silicate-carbonate assemblages from the Nolans Bore P-REE-Th Deposit, Northern Territory, Australia. *The Canadian Mineralogist*, **56(3)**, 331-354.

Arzamastsev, A. A., Glaznev, V. N., Raevsky, A. B. and Arzamastseva, L. V. 2000. Morphology and internal structure of the Kola Alkaline intrusions, NE Fennoscandian Shield: 3D density modelling and geological implications. *Journal of Asian Earth Sciences*, **18(2)**, 213-228.

Banks, G. J., Walter, B. F., Marks, M. A. and Siegfried, P. R. 2019. A workflow to define, map and name a carbonatite-or alkaline igneous-associated REE-HFSE mineral system: A case study from SW Germany. *Minerals*, **9(2)**, https://www.mdpi.com/2075-163X/9/2/97

Beard, C. D., Goodenough, K. M., Borst, A. M., Wall, F., Siegfried, P. R., Deady, E. A., Pohl, C., Hutchinson, W., Finch, A., Walter, B. F., Elliot, H. and Brauch, K. 2023. Alkaline-silicate REE-HFSE systems. *Economic Geology*, **118(1)**, 177-208.

Braunger, S., Marks, M. A. W., Walter, B. F., Neubauer, R., Reich, R., Wenzel, T., Parsapoor, A. and Markl, G. 2018. The petrology of the Kaiserstuhl Volcanic Complex, SW Germany: the importance of metasomatized and oxidized lithospheric mantle for carbonatite generation. *Journal of Petrology*, **59(9)**, 1731-1762.

Brett, R. C., Russell, J. K., Andrews, G. D. M. and Jones, T. J. 2015. The ascent of kimberlite: Insights from olivine. *Earth and Planetary Science Letters*, **424**, 119-131.

Broom-Fendley, S., Brady, A. E., Horstwood, M. S., Woolley, A. R., Mtegha, J., Wall, F., Dawes, W. and Gunn, G. 2017. Geology, geochemistry and geochronology of the Songwe Hill carbonatite, Malawi. *Journal of African Earth Sciences*, **134**, 10-23.

Broom-Fendley, S., Siegfried, P. R., Wall, F., O'Neill, M., Brooker, R. A., Fallon, E. K., Pickles, J. and Banks, D. A. 2021. The origin and composition of carbonatite-derived carbonate-bearing fluorapatite deposits. *Mineralium Deposita*, **56(5)**, 863-884.

Browne, B. and Szramek, L. 2015. Rates of magma ascent and storage, 203-214. *In*: H. Sigurdsson, (Ed.), *The Encyclopedia of volcanoes*. Academic Press, Cambridge, Mass., USA.

Bühn, B., Dörr, W. and Brauns, C. M. 2001. Petrology and age of the Otjisazu carbonatite complex, Namibia: implications for the pre-and synorogenic Damaran evolution. *Journal of African Earth Sciences*, **32(1)**, 1-17.

Burke, K., Ashwal, L. D. and Webb, S. J. 2003. New way to map old sutures using deformed alkaline rocks and carbonatites. Geology, **31(5)**, 391-394.

Campeny, M., Mangas, J., Melgarejo, J. C., Bambi, A., Alfonso, P., Gernon, T. and Manuel, J. 2014. The Catanda extrusive carbonatites (Kwanza Sul, Angola): an example of explosive carbonatitic volcanism. *Bulletin of Volcanology*, **76(4)**, 818.

Caricchi, L., Simpson, G. and Schaltegger, U. 2014. Zircons reveal magma fluxes in the Earth's crust. *Nature*, **511(7510)**, 457-461.

Caricchi, L., Simpson, G. and Schaltegger, U. 2016. Estimates of volume and magma input in crustal magmatic systems from zir-

con geochronology: the effect of modeling assumptions and system variables. *Frontiers in Earth Science*, **4**, https://doi.org/10.3389/feart.2016.00048

Casquet, C., Pankhurst, R. J., Galindo, C., Rapela, C., Fanning, C. M., Baldo, E., Dahlquist, J., Cascado, J. and Colombo, F. 2008. A deformed alkaline igneous rock–carbonatite complex from the Western Sierras Pampeanas, Argentina: Evidence for late Neoproterozoic opening of the Clymene Ocean? *Precambrian Research*, **165(3-4)**, 205-220.

Chakhmouradian, A. R., Reguir, E. P., Zaitsev, A. N., Coueslan, C., Xu, C., Kynický, J., Mumin, H. and Yang, P. 2017. Apatite in carbonatitic rocks: Compositional variation, zoning, element partitioning and petrogenetic significance. *Lithos*, **274**, 188-213.

Chandra, J., Paul, D., Stracke, A., Chabaux, F. and Granet, M. 2019. The origin of carbonatites from Amba Dongar within the Deccan large igneous province. *Journal of Petrology*, **60(6)**, 1119-1134.

Choudhuri, R. and Banerji, K. C. 1976. On the occurrence, emplacement and origin of the apatite deposits of Kasipatnam in Visakhapatnam district, Andhra Pradesh. *Proceedings of the Indian National Science Academy*, **42**, 387-406.

Corner, B. 2000. Crustal framework of Namibia derived from magnetic and gravity data. *Communications of the Geological Survey of Namibia*, **12**, 13-19.

Crisp, J. A. 1984. Rates of magma emplacement and volcanic output. *Journal of Volcanology and Geothermal Research*, **20(3-4)**, 177-211.

Dawson, J. B. 1962. The geology of Oldoinyo Lengai. *Bulletin Volcanologique*, **24(1)**, 349-387.

Drüppel, K., Wagner, T. and Boyce, A. J. 2006. Evolution of sulfide mineralization in ferrocarbonatite, Swartbooisdrif, Northwestern Namibia: constraints from mineral compositions and sulfur isotopes. *The Canadian Mineralogist*, **44(4)**, 877-894.

Edahbi, M., Plante, B., Benzaazoua, M., Kormos, L. and Pelletier, M. 2018. Rare earth elements (La, Ce, Pr, Nd, and Sm) from a carbonatite deposit: Mineralogical characterization and geochemical behavior. *Minerals*, **8(2)**, https://doi.org/10.3390/min8020055

Elliott H. A. L., Wall. F., Chakhmouradian A. R., Siegfried P. R., Dahlgren, S., Weatherley, S., Finch, A. A., Marks, M. A. W., Dowman, E. and Deady, E. 2018. Fenites associated with carbonatite complexes: A review. *Ore Geology Reviews*, **93**, 38–59

Emeleus, C. H., Bell, B. R. and MacGregor, A. G. 2005. *The Palaeogene volcanic districts of Scotland*, **3**. British Geological Survey, Nottingham, UK, 212 pp.

England, R. W. 1988. The early Tertiary stress regime in NW Britain: evidence from the patterns of volcanic activity, 381-389. *In*: A. C. Morton and L. M. Parson (Eds), Early Tertiary Volcanism and the Opening of the NE Atlantic. *Geological Society Special Publications*, **39**, The Geological Society of London, UK.

Epshteyn, Y. M. and Kaban'kov, V. Y. 1984. The depth of emplacement and mineral potential of ultramafic, ijolite, and carbonatite plutons. *International Geology Review*, **26(12)**, 1402-1415.

Eriksson, S. C. 1982. Kimberlites and associated alkaline magmatism, 424-432. *In*: A. J. Tankard, K. A. Eriksson, D. R. Hunter, M. P. A. Jackson, D. K. Hobday and W. E. L. Minter (Eds), *Crustal Evolution of Southern Africa: 3.8 Billion Years of Earth History*. Springer, New York, 524 pp.

Ernst, R. E. and Bell, K. 2010. Large igneous provinces (LIPs) and carbonatites. *Mineralogy and Petrology*, **98(1)**, 55-76.

Frolov, A. A. 1971. Vertical zonation in deposition of ore, as in ultrabasic-alkaline rocks and carbonatites. *International Geology Review*, **13(5)**, 685-695.

Genge, M. J., Price, G. D. and Jones, A. P. 1995. Molecular dynamics simulations of $CaCO_3$-melts to mantle pressures and temperatures: implications for carbonatite magmas. *Earth and Planetary Science Letters*, **131(3-4)**, 225-238.

Giebel, R. J., Gauert, C. D., Marks, M. A., Costin, G. and Markl, G. 2017. Multi-stage formation of REE minerals in the Palabora Carbonatite Complex, South Africa. *American Mineralogist*, **102(6)**, 1218-1233.

Giebel, R. J., Parsapoor, A., Walter, B. F., Braunger, S., Marks, M. A., Wenzel, T. and Markl, G. 2019. Evidence for magma–wall rock interaction in carbonatites from the Kaiserstuhl Volcanic Complex (Southwest Germany). *Journal of Petrology*, **60(6)**, 1163-1194.

Giebel, R. J., Marks, M. A. W., Gauert, C. D. K. and Markl, G. 2019a. A model for the formation of carbonatite-phoscorite assemblages based on the compositional variations of mica and apatite from the Palabora Carbonatite Complex, South Africa. *Lithos*, **324-325**, 89-114.

Goodenough, K. M., Deady, E. A., Beard, C. D., Broom-Fendley, S., Elliott, H. A., Van Den Berg, F. and Öztürk, H. 2021. Carbonatites and alkaline igneous rocks in post-collisional settings: storehouses of rare earth elements. *Journal of Earth Science*, **32(6)**, 1332-1358.

Gudelius, D., Marks, M. W., Markl, G., Nielsen, T. F., Kolb, J. and Walter, B. 2023. The origin of ultramafic complexes with melilitolites and carbonatites: a petrological comparison of the Gardiner (E Greenland) and Kovdor (Russia) intrusions. *Journal of Petrology*, **64(6)**, https://doi.org/10.1093/petrology/egad036

Gudmundsson, A. 2002. Emplacement and arrest of sheets and dykes in central volcanoes. *Journal of Volcanology and Geothermal Research*, **116(3-4)**, 279-298.

Hawkesworth, C. J., Cawood, P. A. and Dhuime, B. 2016. Tectonics and crustal evolution. *GSA Today*, **26(9),** 4-11.

Hay, R. L. and O'Neil, J. R. 1983. Carbonatite tuffs in the Laetolil Beds of Tanzania and the Kaiserstuhl in Germany. *Contributions to Mineralogy and Petrology*, **82(4)**, 403-406.

Humphreys-Williams, E. R. and Zahirovic, S. 2021. Carbonatites and global tectonics. *Elements*, **17(5)**, 339-344.

Hurai, V., Blažeková, M., Huraiová, M., Siegfried, P. R., Slobodník, M. and Konečný, P. 2021. Thermobarometric and geochronologic constraints on the emplacement of the Neoproterozoic Evate carbonatite during exhumation of the Monapo granulite complex, Mozambique. *Lithos*, **380**, https://doi.org/10.1016/j.lithos.2020.105883

Ilyinskaya, E., Schmidt, A., Mather, T. A., Pope, F. D., Witham, C., Baxter, P., Johannsson, T., Pfeffer, M., Barsotti, S., Singh, A., Sanderson, P., Bergsson, B., MacCormmick-Kilbride, B., Donovan, A., Peters, N., Oppenheimer, C. and Edmonds, M. 2017. Understanding the environmental impacts of large fissure eruptions: Aerosol and gas emissions from the 2014–2015 Holuhraun eruption (Iceland). *Earth and Planetary Science Letters*, **472**, 309-322.

Jones, A. P., Genge, M. and Carmody, L. 2013. Carbonate melts and carbonatites. *Reviews in Mineralogy and Geochemistry*, **75(1)**, 289-322.

Kavanagh, J. L., Burns, A. J., Hazim, S. H., Wood, E. P., Martin, S. A., Hignett, S. and Dennis, D. J. 2018. Challenging dyke ascent models using novel laboratory experiments: Implications for reinterpreting evidence of magma ascent and volcanism. *Journal of Volcanology and Geothermal Research*, **354**, 87-101.

Keller, J. and Krafft, M. 1990. Effusive natrocarbonatite activity of Oldoinyo Lengai, June 1988. *Bulletin of Volcanology*, **52(8)**, 629-645.

Khan, A., Faisal, S., Ullah, Z., Ali, L., Ghaffari, A., Nawab, J. and Rashid, M. U. 2021. Pyrochlore-group minerals from the Loe-Shilman Carbonatite Complex, NW Pakistan: implications for evolution of carbonatite system. *Periodico di Mineralogia*, **90(2)**, 277-287.

Kogarko, L. N., Konova, V. A., Orlova, M. P. and Woolley, A. R. 1995. *Alkaline Rocks and Carbonatites of the World - Part Two: Former USSR*. Springer, Dordrecht, Netherlands, 226 pp.

Kono, Y., Kenney-Benson, C., Hummer, D., Ohfuji, H., Park, C., Shen, G., Wang, Y., Kavner, A. and Manning, C. E. 2014. Ultralow viscosity of carbonate melts at high pressures. *Nature communications*, **5(1)**, https://doi.org/10.1038/ncomms6091

Ladisic, A., Marks, M. A., Walter, B. F., Giebel, R. J., Beranoaguirre, A. and Markl, G. 2025. Permo-Triassic magmatism in the Damaraland Igneous Province, NW Namibia: The Ondurakorume alkaline-carbonatite complex. *Geochemistry*, **85(3)**, https://doi.org/10.1016/j.chemer.2025.126287

Le Bas, M. J. 1987. Nephelinites and carbonatites, 53-83. *In*: J. G. Fitton and B. G. J. Upton (Eds), Alkaline Igneous Rocks. *Geological Society Special Publications*, **30**, The Geological Society of London, UK.

Magee, C., Jackson, C. A. L. and Schofield, N. 2013. The influence of normal fault geometry on igneous sill emplacement and morphology. *Geology*, **41(4)**, 407-410.

Matton, G. and Jébrak, M. 2014. The “Eye of Africa” (Richat dome, Mauritania): An isolated Cretaceous alkaline–hydrothermal

complex. *Journal of African Earth Sciences*, **97**, 109-124.

Mariano, A. N. 1989. Cathodoluminescence emission spectra of rare earth element activators in minerals. In. Geochemistry and mineralogy of Rare Earth Elements. *Reviews in Mineralogy*, **21**, 339-348.

Millonig, L. J., Gerdes, A. and Groat, L. A. 2012. U–Th–Pb geochronology of meta-carbonatites and meta-alkaline rocks in the southern Canadian Cordillera: a geodynamic perspective. *Lithos*, **152**, 202-217.

Mitchell, R. H. 2005. Carbonatites and carbonatites and carbonatites. *The Canadian Mineralogist*, **43(6)**, 2049-2068.

Mitchell, R., Chudy, T., McFarlane, C. R. and Wu, F. Y. 2017. Trace element and isotopic composition of apatite in carbonatites from the Blue River area (British Columbia, Canada) and mineralogy of associated silicate rocks. *Lithos*, **286**, 75-91.

Nash, W. P. 1972. Apatite-calcite equilibria in carbonatites: chemistry of apatite from Iron Hill, Colorado. *Geochimica et Cosmochimica Acta*, **36(12)**, 1313-1319.

O'Driscoll, B., Troll, V. R., Reavy, R. J. and Turner, P. 2006. The Great Eucrite intrusion of Ardnamurchan, Scotland: Re-evaluating the ring-dike concept. *Geology*, **34(3)**, 189-192.

Panda, N. K., Rao, A. Y., Kumar, K. R., Mohanty, R. and Parihar, P. S. 2015. Anomalous REE concentration in carbonate–phosphate bearing phases from Narasimharajapuram area, Visakhapatnam district, Andhra Pradesh. *Current Science*, **109(5)**, 860-862.

Pandur, K., Ansdell, K. M. and Kontak, D. J. 2015. Graphic-textured inclusions in apatite: Evidence for pegmatitic growth in a REE-enriched carbonatitic system. *Geology*, **43(6)**, 547-550.

Paul, D., Chandra, J. an Halder, M. 2020. Proterozoic alkaline rocks and carbonatites of Peninsular India: a review. *Episodes*, **43(1)**, 249-277.

Petrovsky, M. N., Savchenko, E. A. and Kalachev, V. Y. 2012. Formation of eudialyte-bearing phonolite from Kontozero carbonatite paleovolcano, Kola Peninsula. *Geology of Ore Deposits*, **54(7),** 540-556.

Plant, J. A., Whittaker, A., Demetriades, A., De Vivo, B. and Lexa, J. 2005. The geological and tectonic framework of Europe. *In*: *Geochemical Atlas of Europe*, **Part 1**. Geological Survey of Finland, Espoo, http://weppi.gtk.fi/publ/foregsatlas/article.php?id=4

Putirka, K. D. 2017. Down the crater: where magmas are stored and why they erupt. *Elements*, **13(1)**, 11-16.

Rao, A. T. 1976. Study of the apatite-magnetite veins near Kasipatnam, Visakhapatnam district, Andhra Pradesh, India. *Tschermaks mineralogische und petrographische Mitteilungen*, **23(2)**, 87-103.

Rapprich, V., Walter, B. F., Kopačková-Strnadová, V., Kluge, T., Čejková, B., Pour, O., Hora, J., Kynicky, J. and Magna, T. 2024. Gravitational collapse of a volcano edifice as a trigger for explosive carbonatite eruption? *GSA Bulletin*, **136(5-6)**, 2291-2304.

Raza, M., Giebel, R. J., Staude, S., Beranoaguirre, A., Kolb, J., Markl, G. and Walter, B. F. 2025. The magmatic to post-magmatic evolution of the Nooitgedacht Carbonatite Complex, South Africa. *Geochemistry*, **85(1),** https://doi.org/10.1016/j.chemer. 2025.126249

Reid, D. L., Cooper, A. F., Rex, D. C. and Harmer, R. E. 1990. Timing of post–Karoo alkaline volcanism in southern Namibia. *Geological Magazine*, **127(5)**, 427-433.

Rosatelli, G., Wall, F. and Stoppa, F. 2007. Calcio-carbonatite melts and metasomatism in the mantle beneath Mt. Vulture (Southern Italy). *Lithos*, **99(3-4)**, 229-248.

Samson, I. M., Liu, W. and Williams-Jones, A. E. 1995. The nature of orthomagmatic hydrothermal fluids in the Oka carbonatite, Quebec, Canada: Evidence from fluid inclusions. *Geochimica et Cosmochimica Acta*, **59(10)**, 1963-1977.

Schmidt, M. W., Giuliani, A. and Poli, S. 2024. The origin of carbonatites—combining the rock record with available experimental constraints. *Journal of Petrology*, **65(10)**, https://doi.org/10.1093/petrology/egae105

Scogings, A. J. and Forster, I. 1989. Gneissose carbonatites in the Bull's Run complex, Natal. *South African Journal of Geology*, **92(1)**, 1-10.

Shu, X. and Liu, Y. 2019. Fluid inclusion constraints on the hydrothermal evolution of the Dalucao Carbonatite-related REE deposit, Sichuan Province, China. *Ore Geology Reviews*, **107**, 41-57.

Simandl, G. J. and Paradis, S. 2018. Carbonatites: related ore deposits, resources, foot-

print, and exploration methods. *Applied Earth Science*, **127(4)**, 123-152.

Sparks, R. S. J., Brooker, R. A., Field, M., Kavanagh, J., Schumacher, J. C., Walter, M. J. and White, J. 2009. The nature of erupting kimberlite melts. *Lithos*, **112**, 429-438.

Stoppa, F. and Woolley, A. R. 1997. The Italian carbonatites: field occurrence, petrology and regional significance. *Mineralogy and Petrology*, **59(1)**, 43-67.

Stoppa, F., Pirajno, F., Schiazza, M. and Vladykin, N. V. 2016. State of the art: Italian carbonatites and their potential for critical-metal deposits. *Gondwana Research*, **37**, 152-171.

Tappe, S., Beard, C. D., Borst, A. M., Humphreys-Williams, E. R., Walter, B. F. and Yaxley, G. M. 2025. Kimberlite, carbonatite and alkaline magmatic systems: definitions, origins, and strategic mineral resources. EarthArXiv Preprints, https://eartharxiv.org/repository/view/8658/

Vartiainen, H. and Paarma, H. 1979. Geological characteristics of the Sokli carbonatite complex, Finland. *Economic Geology*, **74(5)**, 1296-1306.

Vasyukova, O. V. and Williams-Jones, A. E. 2022. Carbonatite metasomatism, the key to unlocking the carbonatite-phoscorite-ultramafic rock paradox. *Chemical Geology*, **602**, https://doi.org/10.1016/j.chemgeo.2022.120888

Verwoerd, W. J. 1967. The carbonatites of South Africa and South West Africa. *Handbook of the Geological Survey of South Africa*, **6**, Government Printer, Pretoria, South Africa, 452 pp.

Von Knorring, O. And Du Bois, C. G. B. 1961. Carbonatitic lava from Fort Portal area in western Uganda. *Nature*, **192(4807)**, 1064-1065.

Walter, B. F., Parsapoor, A., Braunger, S., Marks, M. A. W., Wenzel, T., Martin, M. and Markl, G. 2018. Pyrochlore as a monitor for magmatic and hydrothermal processes in carbonatites from the Kaiserstuhl volcanic complex (SW Germany). *Chemical Geology*, **498**, 1-16.

Walter, B. F., Steele-MacInnis, M., Giebel, R. J., Marks, M. A. and Markl, G. 2020. Complex carbonate-sulfate brines in fluid inclusions from carbonatites: Estimating compositions in the system H_2O-Na-K-CO_3-SO_4-Cl. *Geochimica et Cosmochimica Acta*, **277**, 224-242.

Walter, B. F., Giebel, R. J., Steele-MacInnis, M., Marks, M. A., Kolb, J. and Markl, G. 2021. Fluids associated with carbonatitic magmatism: A critical review and implications for carbonatite magma ascent. *Earth-Science Reviews*, **215**, https://doi.org/10.1016/j.earscirev. 2021.103509

Walter, B. F., Giebel, J., Marlow, A. G., Siegfried, P. R., Marks, M., Markl, G., Palmer, M. and Kolb, J. 2022. The Keishöhe carbonatites of southwestern Namibia–the post-magmatic role of silicate xenoliths on REE mobilisation. *Communications of the Geological Survey of Namibia*, **25**, 1-31.

Walter, B. F., Giebel, R. J., Siegfried, P. R., Gudelius, D. and Kolb, J. 2023. The eruption interface between carbonatitic dykes and diatremes – The Gross Brukkaros volcanic field Namibia. *Chemical Geology*, **621**, https://doi.org/10.1016/j.chemgeo. 2023.121344

Wimmenauer, W. 2003. Geologische Karte von Baden-Württemberg, 1: 25.000 – Erläuterungen zum Blatt Kaiserstuhl. Landesamt für Geologie, Rohstoffe und Bergbau Baden-Württemberg, Freiburg im Breisgau, Germany, 280 pp.

Wooley, A. R. 1987. *Alkaline rocks and carbonatites of the World. 1. North and South America.* Chapman & Hall, London, UK, 141 pp.

Woolley, A. R. 2001. *Alkaline Rocks and Carbonatites of the World. Part 3: Africa*. The Geological Society of London., UK, 384 pp.

Woolley, A. R. 2019. *Alkaline rocks and carbonatites of the world, Part 4: Antarctica, Asia and Europe (excluding the former USSR), Australasia and Oceanic Islands*. The Geological Society of London, UK, 562 pp.

Woolley, A. R. and Church, A. A. 2005. Extrusive carbonatites: a brief review. *Lithos*, **85(1-4)**, 1-14.

Woolley, A. R. and Kjarsgaard, B. A. 2008. Paragenetic types of carbonatite as indicated by the diversity and relative abundances of associated silicate rocks: evidence from a global database. *The Canadian Mineralogist*, **46(4)**, 741-752.

Yaxley, G. M., Kjarsgaard, B. A. and Jaques, A. L. 2021. Evolution of carbonatite magmas in the upper mantle and crust. *Elements*, **17(5)**, 315-320.

Yaxley, G. M., Anenburg, M., Tappe, S., Decree, S. and Guzmics, T. 2022. Carbonatites: classification, sources, evolution, and emplacement. *Annual Review of Earth and Planetary Sciences*, **50(1)**, 261-293.